Alexandria Engineering Journal (2022) 61, 8069–8088

HOSTED BY ELSEVIER

Alexandria University

Alexandria Engineering Journal

www.elsevier.com/locate/aej
www.sciencedirect.com

# An improved metaheuristic method for simultaneous network reconfiguration and distributed generation allocation

**Truong Hoang Bao Huy** [a], **Thanh Van Tran** [a], **Dieu Ngoc Vo** [b,c,*], **Ho Thi Thao Nguyen** [d]

[a] *Institute of Engineering and Technology, Thu Dau Mot University, Binh Duong Province, Viet Nam*
[b] *Department of Power Systems, Ho Chi Minh City University of Technology (HCMUT), 268 Ly Thuong Kiet Street, District 10, Ho Chi Minh City, Viet Nam*
[c] *Vietnam National University Ho Chi Minh City, Linh Trung Ward, Thu Duc District, Ho Chi Minh City, Viet Nam*
[d] *FPT University, Hanoi, Viet Nam*

Received 10 June 2021; revised 5 January 2022; accepted 20 January 2022
Available online 29 January 2022

**KEYWORDS**

Distributed generations;
Chaotic local search;
Network reconfiguration;
Radial distribution networks;
Search group algorithm

**Abstract** A new chaotic search group algorithm (CSGA) is proposed in this study for simultaneous network reconfiguration and allocation of distributed generation (SNR-DG) problem with the objective of minimum real power loss in the radial distribution network (RDN). The CSGA is an improved metaheuristic algorithm, in which a chaotic local search strategy is incorporated with the original SGA, to enhance its search performance. The proposed CSGA was studied on 33-, 69-, 84- and 118-bus RDNs with three load levels. After SNR-DG application, the voltage profile and real power loss of the system had enhanced significantly. The outcomes yielded by CSGA were compared with those obtained from the original SGA and other techniques depicted in the literature. The comparative findings revealed that CSGA yielded better solution quality than SGA and other techniques. Hence, CSGA is the best technique to address the SNR-DG problem in RDNs.



## 1. Introduction

The radial distribution network (RDN) is integral in power systems for transferring electricity to consumers. Nevertheless, optimal RDN planning and operation appear to pose some challenges to the planners and executioners [1]. Power loss reduction (PLR) is one of the critical factors to optimally operate the system [2]. Apparently, the integration of simultaneous network reconfiguration and distributed generation allocation (SNR-DG) is effective in enhancing the performance of RDNs [3]. Network reconfiguration (NR) refers to the status changing process of tie switches (typically opened) and sectionalizing switches (typically closed) for optimum RDN restructuring.

* Corresponding author.
E-mail address: vndieu@hcmut.edu.vn (D. Ngoc Vo).

Peer review under responsibility of Faculty of Engineering, Alexandria University.

https://doi.org/10.1016/j.aej.2022.01.056

Meanwhile, escalating demand for electricity and cost-effective generation, environmental concerns, and cutting-edge technologies have expanded distributed generations (DGs) integration. This approach has minimized operating costs, transmission congestion, and system power loss; while enhancing voltage profile and reliability. However, studies pertaining to NR and DG allocation have been in isolation, mainly because the NR turns into a more intricate aggregation problem upon the incorporation of DGs allocation. However, SNR-DG in RDN may address challenges and offer more benefits.

Over the past two decades, many researchers have been devoted to initiating a broad range of artificial intelligence (AI), analytical, and metaheuristic approaches to address NR problem [4]. Some analytical techniques proposed to address NR are interchange switch [5], open-all switch [6], and close-all switch [7] strategies. Despite the short computation time and easy implementation, these analytical approaches failed to perform in large scale and intricate conditions. As for the biological/physical-inspired AI and metaheuristic approaches, including particle swarm optimization (PSO) [8], genetic algorithm (GA) [9], harmony search algorithm (HSA) [10], fireworks algorithm (FWA) [11], and cuckoo search algorithm (CSA) [12], which were proposed to solve NR problem upon considering power quality and reliability based objectives (e.g., power loss). In particular, metaheuristic techniques have been reported to address the optimization problems with exceptional outcomes [13,14].

In recent years, DG units have been widely connected to RDNs stemming from environmental concerns, electricity deregulation, and fossil fuel depletion. Integration of DGs has displayed significant impacts on RDN operation [15]. Despite their studies in isolation, simultaneous allocations of both NR and DG may generate the sought solution [16]. An improved equilibrium optimization algorithm (IEOA) has been applied by Shaheen et al. [3] to handle the optimal incorporation of DG units and NR. The 33- and 69-bus networks were deployed to validate the proposed approach at three load levels, in which its superiority was verified. A big-bang crunch algorithm [16] was initiated to solve multi-objective optimal NR and DGs allocation in RDNs. Optimal DG locations were omitted in the study. Next, Rao et al. [17] used an HSA-based algorithm to overcome the NR issue in the presence of DGs for PLR. The locations of DGs were identified based on the loss sensitivity factor. In another study, PSO and grey wolf optimizer were combined to solve NR with DGs installation in large-scale networks [18]. Mohamed et al. [19] formulated an FWA to enhance voltage stability and PLR based on NR and DGs installation, whereby buses with the least voltage stability index were selected for DGs allocation. Meanwhile, an adaptive CSA [20] successfully solved NR with a DG placement to decrease both voltage stability index and power loss. In the study, radial network constraint was determined based on graph theory. A shuffled frogs leaping method was deployed Onlam et al. [21] to seek optimal NR, as well as DGs sizes and locations, for 33- and 69-bus systems for several case studies with two objectives: better voltage profile and lower system loss. Next, an electromagnetism-based approach was implemented for NR with DG placement to maximize PLR [22]. Tolabi et al. [23] applied a hybrid fuzzy-bees approach to handle multi-objective NR with DGs allocation to enhance feeder load balance and voltage profile while maximizing PLR. The HSA-PSO hybrid approach was deployed in an artificial bee colony to overcome the NR and placements of DGs and shunt capacitors for PLR maximization [24]. To achieve power loss minimization, a modified plant growth simulation algorithm had been proposed for NR with DGs [25], whereby DGs positions were found based on sensitivity analysis. A heuristic method was proposed by Bayat et al. [26] for NR and DGs placement to decrease losses. A sine-cosine algorithm, in combination with levy flights, was proposed to address NR with DGs integration in 33- and 69-bus RDNs to lower voltage stability index and power loss [27]. The simultaneous optimal NR and DGs output were solved using the firefly (FF) method in [28] for 33-, 69-, and 118-bus systems. In fact, only a handful of studies have looked into NR and DGs installation as a combinational optimization problem. Moreover, most previous studies have not investigated the SNR-DG problem on a large-scale RDN. The SNR-DG is effective to enhance the reliability, performance, and quality of RDNs. As the combined problem may comprise of multiple variables and constraints, it is crucial to develop a method that can effectively address the intricate optimization problem.

Search group algorithm (SGA) has been developed by Goncalves et al. [29], which is a promising optimization method. For benchmark problems in topology optimization, SGA has proven better performance than genetic algorithm (GA), particle swarm algorithm (PSO), harmony search (HS) and firefly algorithm (FA) [29]. Since SGA has stochastic nature, it may get stuck in the local optimum and converge prematurely. To overcome the above disadvantages, chaos-based search algorithms have been developed in the literature. Chaotic search strategy has been integrated into many metaheuristic optimization algorithms such as cuckoo search (CS) [30,31], krill herd (KH) [32,33], symbiotic organisms search (SOS) [34,35], antlion optimizer (ALO) [36] to enhance the overall search performance of such algorithms. Due to their randomness, non-repetitive and ergodicity nature, chaotic sequences can obtain high effectiveness in the local optimization [35].

Having the above mentioned, this present study proposes a new chaotic search group algorithm (CSGA) to address the SNR-DG problem. It is noteworthy to highlight that the SNR-DG problem is indeed a critical challenge stemming from its intricate, large scale, and non-linear nature. The primary goal of this SNR-DG is PLR while being subjected to several constraints of system operations including radial configuration and bus voltage limitations, power balance, as well as DG and feeder capacity limits. In the proposed CSGA, a chaotic local search (CLS) strategy was deployed to enhance accuracy and convergence speed, while avoiding local trapping. The CSGA was tested on IEEE 33-, 69-, 84-, and 118-bus RDNs with three load levels. Later, the CSGA outcomes were compared with findings retrieved using other techniques outlined in the literature to confirm its superiority in handling the SNR-DG problem.

The key contributions of the present work can be outlined as follows:

- A new CSGA was developed by integrating the CLS strategy into the original SGA.
- The proposed CSGA was successfully applied to the SNR-DG problem in 33-, 69-, 84-, and 118-bus RDNs under three load levels.

- Analysis results indicated that the implementation of SNR-DG has effectively improved the power losses and voltage profiles of systems. For 33-, 69-, 84-, and 118-bus RDNs, CSGA yielded power loss reductions at nominal load condition of 73.1204%, 84.2867%, 35.6577%, and 64.0171%, respectively.
- The comparative yields revealed the superiority of CSGA to other algorithms for solution quality for all case studies. As for the 118-bus large-scale RDN at normal load level, CSGA obtained the best real power loss (467.0906 kW) in comparison to SGA (742.9589 kW), moth search (644.3031 kW), monarch butterfly optimization (853.5588 kW), and ant colony optimization (854.8006 kW).

This paper is organized as given in the following: Section 2 outlines the SNR-DG formulation, while the proposed CSGA is described in Section 3. Section 4 depicts CSGA deployment to the SNR-DG problem. Sections 5 and 6 present the simulation outcomes and the study conclusions, respectively.

## 2. Problem formulation

The objective function ($OF$) of the SNR-DG problem is to minimize real power loss ($P_L$) in RDN while sustaining all constraints. The SNR-DG problem is expressed below:

$$OF = \text{Min}(P_L) = \text{Min}\left(\sum_{k=1}^{N_L} R_k I_k^2\right) \tag{1}$$

where $R_k$ denotes the resistance of $k^{\text{th}}$ branch, $I_k$ signifies the current passing through that branch, whereas $N_L$ represents the number of branches in RDN.

The $OF$ is subjected to the operational constraints outlined as follows:

i. *Power balance:* both real and reactive powers of the system must be balanced:

$$P_{Slack} + \sum_{i=1}^{N_{DG}} P_{DG,i} = \sum_{j=1}^{N_B} P_{D,j} + \sum_{k=1}^{N_L} P_{L,k} \tag{2}$$

$$Q_{Slack} + \sum_{i=1}^{N_{DG}} Q_{DG,i} = \sum_{j=1}^{N_B} Q_{D,j} + \sum_{k=1}^{N_L} Q_{L,k} \tag{3}$$

where $P_{Slack}$ and $Q_{Slack}$ refer to active and reactive power outputs of slack bus, respectively; $P_{DG,i}$ and $Q_{DG,i}$ denote active and reactive power outputs of $i^{\text{th}}$ DG unit, respectively; $N_{DG}$ reflects the total number of DG units to be connected; $P_{D,j}$ and $Q_{D,j}$ signify active and reactive power demands at $j^{\text{th}}$ bus, respectively; $N_B$ represents the total number of buses; while $P_{L,k}$ and $Q_{L,k}$ depict active and reactive power losses in $k^{\text{th}}$ branch, respectively.

ii. *Bus voltage limits:* The bus voltage is bound by lower and upper limits:

$$V_{\min,i} \leqslant V_i \leqslant V_{\max,i}; \quad i = 1, \ldots, N_B \tag{4}$$

where $V_{\min,i}$ and $V_{\max,i}$ refer to voltage limits at the $i^{\text{th}}$ bus.

iii. *Feeder capacity limits:* Flow of current in transmission lines must be below the maximum value:

$$|I_k| \leqslant |I_{\max,k}|; \quad k = 1, \ldots, N_L \tag{5}$$

where $I_{\max,k}$ signifies the permissible maximum flow of current through $k^{\text{th}}$ branch.

iv. *DG capacity limits:* The DG capacity is bound by its lower and upper limits:

$$P_{DG\min,i} \leqslant P_{DG,i} \leqslant P_{DG\max,i}; \quad i = 1, \ldots, N_{DG} \tag{6}$$

where $P_{DG\min,i}$ and $P_{DG\max,i}$ reflect the limited sizes of $i^{\text{th}}$ DG.

v. *DG penetration limits*: The DGs penetration level to the RDN should be bound by lower and upper limits [19]:

$$0.1 \times \sum_{j=2}^{N_B} P_{D,j} \leqslant \sum_{i=1}^{N_{DG}} P_{DG,i} \leqslant 0.6 \times \sum_{j=2}^{N_B} P_{D,j} \tag{7}$$

vi. *Radial configuration constraint*: Distribution network must ascertain radial configuration and serve all loads after reconfiguration [37,38]:

$$\det(\boldsymbol{A}) = \begin{cases} 1 \text{ or } -1 & \text{(radial system)} \\ 0 & \text{(not radial)} \end{cases} \tag{8}$$

where $\boldsymbol{A}$ is the branch-bus incidence matrix in RDN. $\boldsymbol{A}_{ij} = 1/\text{-}1$ if $i^{\text{th}}$ branch is linked from/to $j^{\text{th}}$ bus, otherwise $\boldsymbol{A}_{ij} = 0$.

## 3. Chaotic search group algorithm

The CSGA refers to the enhanced version of the original SGA embedded with a chaotic local search approach. In CSGA, the chaotic local search facilitates the algorithm in exploiting the best solution vicinity to enhance exploitability. By using the chaotic local search strategy, CSGA reaches optimum solution faster and generates better solution quality in solving optimization problems.

### 3.1. Search group algorithm

The SGA is a metaheuristic optimization algorithm proposed in [29]. The SGA offers an exceptional balance between exploitation and exploration of the design domain. During initial optimization iterations, SGA seeks promising areas in the domain (exploration). In the following iterations, SGA seeks the best solution in every promising area (exploitation). Perturbation constant ($\alpha$) refers to the parameter that controls the SGA optimization process, while the mutation step creates new solutions for the current search group. The new solutions are created by a few individuals from the population known as the search group.

First, an initial population is created in a random manner. The population of $n_{pop}$ individuals in SGA is represented by $\boldsymbol{P} = [P_1, \ldots, P_{n_{pop}}]^T$. Next, all individuals of the population are assessed, wherein $n_g$ individuals are selected from population

$\boldsymbol{P}$ to generate a search group $\boldsymbol{R}$ via standard tournament selection. The search group is mutated at each iteration to enhance SGA global searchability, in which new individuals substitute the $n_{mut}$ search group members, as given in the following:

$$x_{j,mut} = E[\boldsymbol{R}_{:,j}] + t\varepsilon\sigma[\boldsymbol{R}_{:,j}]; \quad \text{for } j = 1, ..., n, \tag{9}$$

where $x_{j,mut}$ refers to $j^{\text{th}}$ variable of a mutated individual, $E$ and $\sigma$ denote mean value and standard deviation operators, $\varepsilon$ signifies a convenient random variable, $t$ controls the extent of new individual creation, $\boldsymbol{R}_{:,j}$ indicates $j^{\text{th}}$ column of search group matrix, and $n$ signifies the number of design variables. Search group member replacement probability is dictated by the search group rank aided by inverse tournament selection.

Once the search group is generated and mutated, every search group member generates a family with the following perturbation:

$$x_{j,new} = R_{ij} + \alpha; \quad \text{for } j = 1, ..., n, \tag{10}$$

in which $\alpha$ controls perturbation size. At each iteration of the optimization procedure, SGA is characterized by a decrease in perturbation. The parameter $\alpha$ is updated as below:

**Algorithm 1: Pseudocode of SGA**

**Input:** population size ($n_{pop}$), number of search group member ($n_g$), number of mutations ($n_{mut}$), perturbation factor ($\alpha$), and maximum number of iterations ($maxIter$).

**Output:** Optimal solution $x^* = \boldsymbol{R}_{1,:}$

**Step 1: Initialization**
$x_1, x_2, \ldots, x_{npop}$ = initialization()
**for** $i = 1 : n_{pop}$
  $OF_i$ = fitness($x_i$)
**end for**
Sort all individuals of population $\boldsymbol{P}$
**Step 2: Initial search group selection**
Create the initial search group $\boldsymbol{R}^m$ by selecting $n_g$ individuals from population $\boldsymbol{P}$.
**for** $Iter = 1 : maxIter$
  **Step 3: Mutation of the search group**
  index = reversetournament()
  **for** $j = 1 : n_{mut}$
    $x_{mut} = \boldsymbol{R}_{index(j)}$
    $x_{new}$ = mutation($x_{mut}$)
  **end for**
  **Step 4: Generation of the families**
  **for** $i = 1 : n_g$
    $x_{i,leader} = \boldsymbol{R}_i$
    $\boldsymbol{F}_i$ = familygeneration($x_{i,leader}$)
  **end for**
  **Step 5: Selection of the new search group**
  *% Global phase %*
  Sort each family
  Form search group $\boldsymbol{R}^{m+1}$ by selecting the best member of each family
  *% Local phase %*
  Sort members in all families
  Form search group $\boldsymbol{R}^{m+1}$ by selecting the best $n_g$ members among all families
  $\alpha^{m+1} = b\alpha^m$
**end for**
Return $x^* = \boldsymbol{R}_{1,:}$

**Fig. 1** Pseudocode of the SGA.

$$\alpha^{m+1} = b\alpha^m \tag{11}$$

where $m$ signifies iteration, while $b$ denotes an SGA parameter. The minimum value for $\alpha^k$ is as follows: if $\alpha^m < \alpha^{\min}$, then $\alpha^m = \alpha^{\min}$. A prominent feature of SGA refers to the creation of more individuals with better search group member quality. Lastly, the best member from each family at the global stage generates the new search group. Nevertheless, the selection scheme is adjusted at the local stage, whereby the best $n_g$ individuals from all families create a new search group to exploit the area in the current best design. Fig. 1 presents the pseudocode of the SGA.

**Algorithm 2: Pseudocode of CSGA**

**Input:** population size ($n_{pop}$), number of search group member ($n_g$), number of mutations ($n_{mut}$), perturbation factor ($\alpha$), maximum number of iterations ($maxIter$), and maximum iterations of chaotic local search ($K$).

**Output:** Optimal solution $x^* = \boldsymbol{R}_{1,:}$

```
Step 1: Initialization
x1, x2, …, xnpop = initialization()
for i = 1 : npop
    OFi = fitness(xi)
end for
Sort all individuals of population P
Step 2: Initial search group selection
Create the initial search group R^m by selecting ng individuals from population P.
for Iter = 1 : maxIter
    Step 3: Mutation of the search group
    index = reversetournament()
    for j = 1 : nmut
        xmut = R_index(j)
        xnew = mutation(xmut)
    end for
    Step 4: Generation of the families
    for i = 1 : ng
        xi,leader = Ri
        Fi = familygeneration(xi,leader)
    end for
    Step 5: Selection of the new search group
    % Global phase %
    Sort each family
    Form search group R^(m+1) by selecting the best member of each family
    % Local phase %
    Sort members in all families
    Form search group R^(m+1) by selecting the best ng members among all families
    Step 6: Chaotic local search
    for i = 1 : ng
        Xi = Ri
        Z0 = rand(0,1)
        for k = 1 : K
            Generate Zk using PLCM
            Xik,new = Xik + r(2Zk – 1)
            if fitness(Xik,new) < fitness(Xik)
                Xik = Xik,new
            end if
            r = rand(0,1)×r
        end for
    end for
    α^(m+1) = bα^m
end for
Return x* = R1,:
```

**Fig. 2** Pseudocode of the CSGA.

*3.2. Proposed chaotic search group algorithm*

In this study, the chaotic sequences are incorporated into the CSGA to enhance CSGA search performance and to hinder CSGA from getting stuck in local optimization. The proposed CSGA has two optimization stages. The original SGA is deployed to determine the best solutions in the design domain at the initial stage. Next, a chaotic local search is executed to better exploit the best solutions. The piecewise linear chaotic map (PLCM) was employed to yield the chaotic sequence. The following expresses the initial chaotic sequence variable:

$$Z_0 = rand(0, 1) \tag{12}$$

The next variables of the chaotic sequence based on PLCM are mathematically defined in the following equations [39]:

$$Z_{k+1} = \begin{cases} \frac{Z_k}{p} & Z_k \in (0, p) \\ \frac{(1-Z_k)}{(1-p)} & Z_k \in (p, 1) \end{cases} \tag{13}$$

where $Z_k \in (0, 1)\ \forall k \in \{0, 1, 2, ...\}$ and $p \in (0, 0.5]$.

The chaotic local search is integrated to accelerate the search process for the existing search group members to create better solutions. A new solution is created from the current member of the search group based on the following equation [34]:

$$X_{ik,new} = X_{ik} + r(2Z_k - 1) \tag{14}$$

where $X_{ik,new}$ refers to the new solution position generated from chaotic local search at $k^{\text{th}}$ iteration; $X_{ik}$ reflects $i^{\text{th}}$ member position in the search group at $k^{\text{th}}$ iteration, and $Z_k$ denotes chaotic variable at $k^{\text{th}}$ iteration.

The chaotic search radius ($r$) is determined first and updated in the next iterations, as follows [39]:

$$r = (X_{\max} - X_{\min})/2 \tag{15}$$

$$r^{k+1} = rand(0, 1) \times r^k \tag{16}$$

$X_{ik,new}$ will substitute $X_{ik}$ in the search group if the value of its $OF$ value is better than that of $X_{ik}$. The chaotic local search is executed until maximum iterations of chaotic local search ($K$) is retrieved.

A detailed outline of the CSGA is defined in Fig. 2.

## 4. Implementation of CSGA to SNR-DG problem

*4.1. Initialization*

In CSGA, the initial population is signified by $\boldsymbol{P} = [P_1, ..., P_{n_{pop}}]^T$, where each individual $P_i$ ($i = 1, \ldots, n_{pop}$) includes control variables of opened switches, positions and capacities of DG units:

$$P_i = [SW_1, ..., SW_{N_{SW}}, L_{DG,1}, ..., L_{DG,N_{DG}}, P_{DG,1}, ..., P_{DG,N_{DG}}] \tag{17}$$

Each individual of the initial population is randomly generated within the boundaries:

$$SW_i = round[SW_{\min,i} + rand(0, 1) \times (SW_{\max,i} - SW_{\min,i})], \quad i = 1, ..., N_{SW} \tag{18}$$

$$L_{DG,i} = round[L_{DG\min,i} + rand(0, 1) \times (L_{DG\max,i} - L_{DG\min,i})]; \quad i = 1, ..., N_{DG} \tag{19}$$

$$P_{DG,i} = P_{DG\min,i} + rand(0,1) \times (P_{DG\max,i} - P_{DG\min,i}); \quad i = 1, ..., N_{DG} \tag{20}$$

where $N_{SW}$ indicates the total number of opened switches.

### 4.2. Objective function value

The $OF$ value for each individual of CSGA is calculated as follows:

$$F_T = OF + K_P \sum_{i=1}^{N_B} (V_i - V_i^{\lim})^2 + K_P \sum_{k=1}^{N_L} (I_k - I_k^{\lim})^2 + K_P (PE_{DG} - PE_{DG}^{\lim})^2 \tag{21}$$

in which $K_P$ represents penalty constants for inequality constraint violations. If the dependent variables (bus voltages, feeder capacity, and DGs penetration) violate the constraints, a method is applied to adjust the variables towards to their bound:

$$x^{\lim} = \begin{cases} x_{\min} & \text{if } x < x_{\min} \\ x_{\max} & \text{if } x > x_{\max} \\ x & \text{otherwise} \end{cases} \tag{22}$$

in which $x$ indicates the $V_i$, $I_k$, and $PE_{DG}$ values; $x^{\lim}$ indicates the limitations of $V_i$, $I_k$, and $PE_{DG}$.

### 4.3. Overall procedure

The CSGA deployment for the SNR-DG problem may be outlined as given below:

*Step 1*: Set initial parameters of CSGA ($n_{pop}$, $n_g$, $n_{mut}$, α, $maxIter$, and $K$).

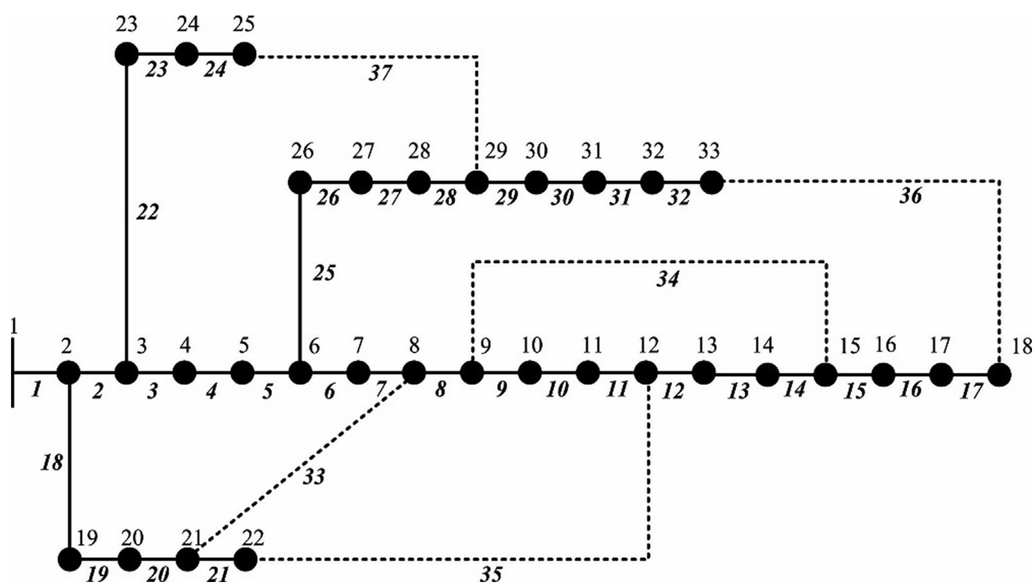


**Fig. 3** The IEEE 33-bus RDN.

**Table 1** Optimal results of CSGA and SGA for 33-bus RDN at three load levels.

| Methods | Item | Load level | | |
|---|---|---|---|---|
| | | Light (0.5) | Normal (1) | Heavy (1.6) |
| Base case | Opened switches | 33-34-35-36-37 | 33-34-35-36-37 | 33-34-35-36-37 |
| | $P_L$ (kW) | 47.07 | 202.66 | 575.31 |
| | $V_{min}$ (p.u) | 0.9583 | 0.9131 | 0.8529 |
| SGA | Opened switches | 8-11-27-32-33 | 10-28-30-33-34 | 10-28-30-33-34 |
| | $P_{DG}$ (MW)/(Bus) | 0.2199/ (7)0.3391/ (15)0.5555/ (30) | 0.8154/ (18)0.8718/ (25)0.5419/ (26) | 0.7324/ (8)1.5028/ (18)1.3312/ (29) |
| | $P_L$ (kW) | 14.4566 | 56.5589 | 152.5012 |
| | PLR (%) | 69.2875 | 72.0941 | 73.4947 |
| | $V_{min}$ (p.u) | 0.9851 | 0.9618 | 0.9500 |
| CSGA | Opened switches | 7-9-14-27-31 | 7-9-14-28-30 | 7-9-14-27-31 |
| | $P_{DG}$ (MW)/(Bus) | 0.2384/ (12)0.3042/ (18)0.5720/ (29) | 0.4697/ (12)1.0213/ (25)0.7380/ (33) | 0.7722/ (12)1.8453/ (29)0.9489/ (33) |
| | $P_L$ (kW) | 13.5232 | 54.4788 | 146.8374 |
| | PLR (%) | 71.2704 | 73.1204 | 74.4791 |
| | $V_{min}$ (p.u) | 0.9867 | 0.9677 | 0.9571 |

*Step 2*: Initialize population $\boldsymbol{P}$ as in Section 4.1. Calculate $OF$ values for $\boldsymbol{P}$ using **equation (21)**;
*Step 3*: Select $n_g$ best solutions from $\boldsymbol{P}$ to form the initial search group $\boldsymbol{R}^m$. Set $Iter = 0$;
*Step 4*: Set $Iter = Iter + 1$;
*Step 5*: Implement mutation phase for $n_{mut}$ individuals based on **equation (9)**;
*Step 6*: Generate families ($\boldsymbol{F}_i$) for each search group member based on **equation (10)**;
*Step 7*: Perform new search group selection in the following manner:
Global stage: choose best solutions of each family to form search group $\boldsymbol{R}^{m+1}$;
Local stage: choose best $n_g$ solutions from all families to form search group $\boldsymbol{R}^{m+1}$.
*Step 8*: Perform the chaotic local search approach to get the best members for the search group;
*Step 9*: Update $\alpha^{m+1}$ based on **equation (11)**;
*Step 10*: If $Iter \geq maxIter$, go to Step 11; if otherwise return to Step 4.
*Step 11*: Solution found: $x^* = \boldsymbol{R}_{1,:}$.

## 5. Simulation results

The proposed CSGA was tested on 33-, 69-, 84-, and 118-bus RDNs to validate its performance. For 33- and 69-bus RDNs, the bus voltage limits were set at 0.95–1.05p.u., while 3 DGs were used with their size ranging at 0–3 kW for DGs distribution. For 84- and 118-bus RDNs, the bus voltage was limited from 0.90p.u. to 1.10p.u., while the system had 5 DGs (for 84-bus RDN) and 7 DGs (for 118-bus RDN) with their sizes from 0 to 5 kW. In this study, three load levels were investigated for the SNR-DG problem: light load level (0.5), normal load level (1.0), and heavy load level (1.6). The CSGA was developed in the MATLAB R2019b. The control parameters of the CSGA included population size ($n_{pop}$), number of search group member ($n_g$), number of mutations ($n_{mut}$), perturbation factor ($\alpha$), maximum number of iterations ($maxIter$), and maximum iterations of chaotic local search ($K$), which were set as follows: $n_{pop} = 50$ and $n_g = 10$ (for 33-, 69-bus, 84-bus RDNs), $n_{pop} = 200$ and $n_g = 40$ (for 118-bus RDN), $n_{mut} = 3$, $\alpha = 2$, $maxIter = 200$, and $K = 10$. For each case, the CSGA was run independently 30 times. Furthermore, Matpower 6.0 was employed to compute power flow analysis. For comparison of results, the original SGA, moth search (MS) [40], monarch butterfly optimization (MBO) [41], and ant colony optimization (ACO) [42] were also deployed to deal with the same problem using the same population size and maximum number of iterations as CSGA.

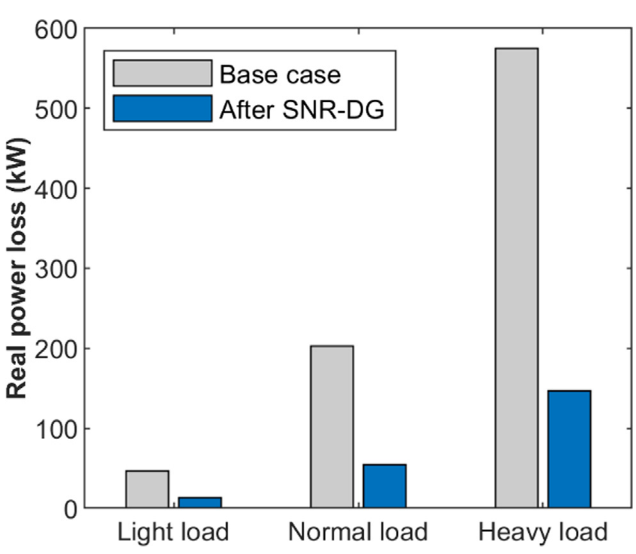


**Fig. 4** Real power loss of 33-bus RDN before and after SNR-DG at three load levels.

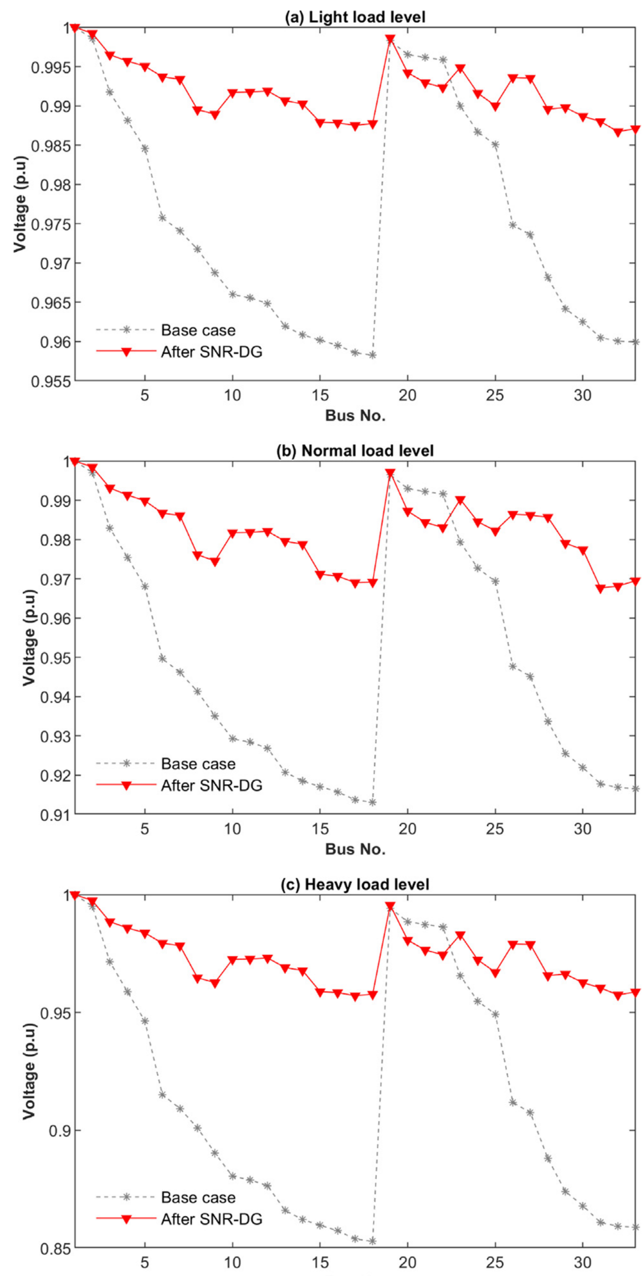


**Fig. 5** Voltage profiles of 33-bus RDN at three load levels.

*5.1. 33-bus RDN*

The IEEE 33-bus RDN refers to a small-scale network with 37 branches, 5 opened switches, and 32 closed switches [43]. The total load demand of the network was 3.72 MW and 2.30 MVAr, while the nominal voltage of the network was 12.66 kV at normal load level. The initially opened switches were 33-34-35-36-37. Fig. 3 illustrates the diagram of the 33-bus RDN.

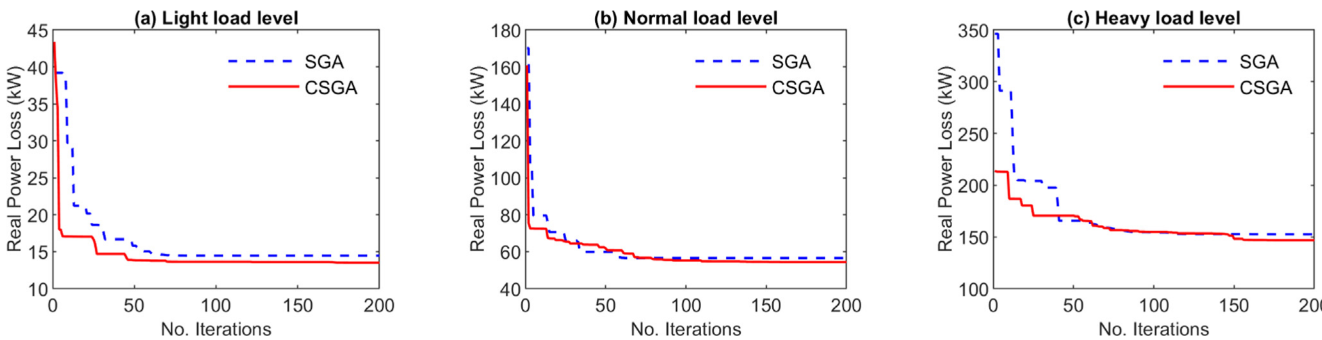


**Fig. 6** Convergence characteristics of CSGA and SGA for 33-bus RDN at three load levels.

**Table 2** Comparative results of CSGA and other methods for 33-bus RDN at three load levels.

| Loading level | Items | Opened switches | Sum $P_{DG}$ (MW) | $P_L$ (kW) | PLR (%) |
|---|---|---|---|---|---|
| Light loading level | Base case | 33-34-35-36-37 | – | 47.068 | – |
| | CSGA | 7-9-14-27-31 | 1.1145 | 13.5232 | 71.2704 |
| | SGA | 8-11-27-32-33 | 1.1145 | 14.4566 | 69.2875 |
| | MS | 11-28-30-33-34 | 1.1133 | 14.1725 | 69.8912 |
| | MBO | 10-14-25-33-34 | 1.0000 | 19.4429 | 58.6944 |
| | ACO | 10-27-31-33-34 | 1.0831 | 14.0210 | 70.2129 |
| | EOA [3] | 6-28-34-35-36 | 1.114 | 15.17 | 67.76 |
| | IEOA [3] | 8-28-32-33-34 | 1.106 | 14.51 | 69.17 |
| | HSA [17] | 7-10-14-28-32 | 0.8898 | 17.78 | 62.22 |
| | FWA [19] | 7-10-14-28-32 | 0.8607 | 16.22 | 65.53 |
| | ISCA [27] | 7-10-14-28-31 | 0.7867 | 16.24 | 65.49 |
| Normal loading level | Base case | 33-34-35-36-37 | – | 202.66 | – |
| | CSGA | 7-9-14-28-30 | 2.2289 | 54.4788 | 73.1204 |
| | SGA | 10-28-30-33-34 | 2.2289 | 56.5589 | 72.0941 |
| | MS | 8-9-27-31-33 | 2.2288 | 58.8080 | 70.9844 |
| | MBO | 7-28-32-33-34 | 2.1662 | 69.5086 | 65.7047 |
| | ACO | 11-27-31-33-34 | 2.1478 | 57.8477 | 71.4582 |
| | EOA [3] | 8-27-33-34-36 | 2.229 | 61.48 | 69.66 |
| | IEOA [3] | 7-10-13-27-31 | 2.228 | 57.40 | 71.67 |
| | HSA [17] | 4-7-10-28-32 | 1.6684 | 73.05 | 63.95 |
| | GA [17] | 7-10-28-32-34 | 1.9633 | 75.13 | 62.92 |
| | RGA [17] | 7-9-12-27-32 | 1.774 | 74.32 | 63.33 |
| | FWA [19] | 7-11-14-28-32 | 1.6841 | 67.11 | 66.89 |
| | ISCA [27] | 7-9-14-28-31 | 1.6912 | 66.81 | 67.03 |
| | FF [28] | 8-9-28-32-33 | 1.7738 | 73.95 | 63.51 |
| Heavy loading level | Base case | 33-34-35-36-37 | – | 575.31 | – |
| | CSGA | 7-9-14-27-31 | 3.5664 | 146.8374 | 74.4791 |
| | SGA | 10-28-30-33-34 | 3.5664 | 152.5012 | 73.4947 |
| | MS | 7-10-13-27-30 | 3.5316 | 162.6813 | 71.7254 |
| | MBO | 7-10-14-27-36 | 3.0000 | 183.5448 | 68.0992 |
| | ACO | 8-27-31-33-34 | 3.5579 | 156.3699 | 72.8223 |
| | EOA [3] | 11-14-28-31-33 | 3.552 | 152.26 | 73.54 |
| | IEOA [3] | 7-9-14-26-31 | 3.566 | 148.42 | 74.19 |
| | HSA [17] | 7-10-14-28-32 | 2.7529 | 194.22 | 66.23 |
| | FWA [19] | 7-10-14-28-32 | 2.7529 | 172.97 | 69.93 |
| | ISCA [27] | 7-9-14-28-31 | 2.9812 | 167.96 | 70.81 |

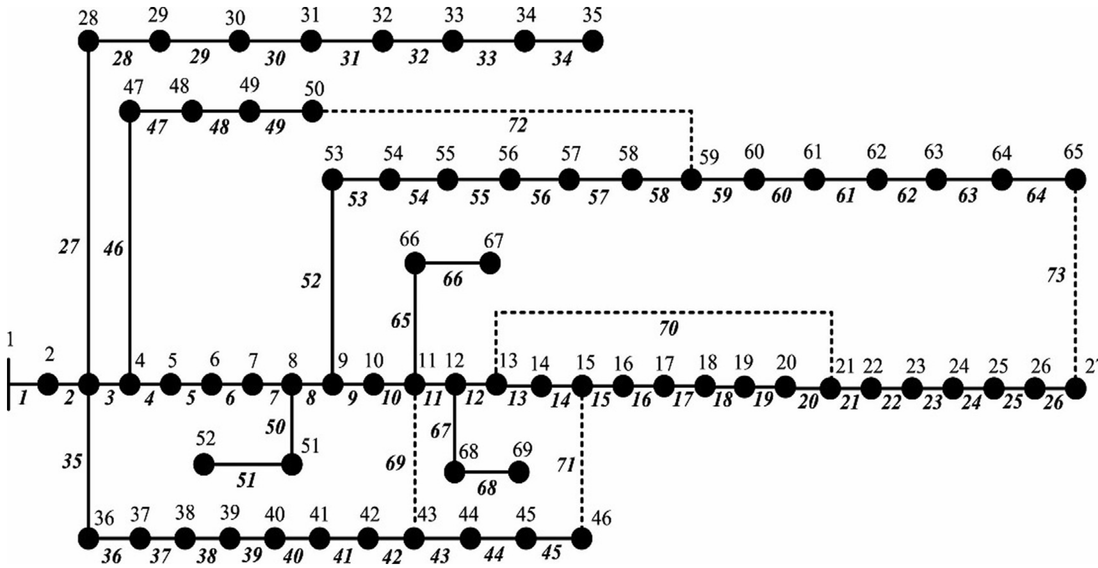

**Fig. 7** The IEEE 69-bus RDN.

**Table 3** Optimal results of CSGA and SGA for 69-bus RDN at three load levels.

| Methods | Item | Load level | | |
|---|---|---|---|---|
| | | Light (0.5) | Normal (1) | Heavy (1.6) |
| Base case | Opened switches | 69-70-71-72-73 | 69-70-71-72-73 | 69-70-71-72-73 |
| | $P_L$ (kW) | 51.61 | 225 | 652.53 |
| | $V_{min}$ (p.u) | 0.9567 | 0.9092 | 0.8445 |
| SGA | Opened switches | 12-18-58-62-69 | 13-56-61-69-70 | 19-55-62-69-71 |
| | $P_{DG}$ (MW)/(Bus) | 0.1755/ (12)0.2675/ (23)0.6976/ (61) | 0.3087/ (21)0.3570/ (27)1.4343/ (61) | 0.8955/ (21)2.2754/ (61)0.4792/ (64) |
| | $P_L$ (kW) | 9.1832 | 38.2621 | 107.7553 |
| | PLR (%) | 82.2053 | 82.9946 | 83.4864 |
| | $V_{min}$ (p.u) | 0.9899 | 0.9813 | 0.9674 |
| CSGA | Opened switches | 14-57-61-69-70 | 14-55-61-69-70 | 14-58-61-69-70 |
| | $P_{DG}$ (MW)/(Bus) | 0.6966/ (61)0.2338/ (64)0.2102/ (66) | 0.4062/ (12)1.4004/ (61)0.4746/ (64) | 2.2330/ (61)0.7557/ (64)0.6613/ (66) |
| | $P_L$ (kW) | 8.7340 | 35.3549 | 93.1537 |
| | PLR (%) | 83.0757 | 84.2867 | 85.7241 |
| | $V_{min}$ (p.u) | 0.9904 | 0.9806 | 0.9683 |

Table 1 tabulates the outcomes obtained from CSGA and SGA for the three load levels. As for the base case, the real power loss of the system at light, nominal, and heavy load levels were 47.07 kW, 202.66 kW, and 575.31 kW, respectively. After the SNR-DG implementation, the power loss from the base case decreased to 13.5232 kW, 54.4788 kW, and 146.8374 kW, corresponding to PLR at 71.2704%, 73.1204%, and 74.4791% at light, normal, and heavy load levels, respectively. Fig. 4 depicts the real power loss of 33-bus RDN before and after SNR-DG implementation. Fig. 5 portrays the voltage profiles of all load levels. Apparently, the minimum voltage magnitude had enhanced from 0.9583p.u., 0.9131p.u., and 0.8529p.u. (base case) to 0.9867p.u., 0.9677p.u., and 0.9571p.u. at light, normal, and heavy load levels, respectively. Hence, the SNR-DG implementation using CSGA had significantly impacted PLR and voltage profile enhancement of the system. Referring to Table 1, the real power loss portrayed by CSGA had been respectively lower than that from SGA for all load levels. As depicted in Fig. 6, the convergence characteristics of CSGA were better

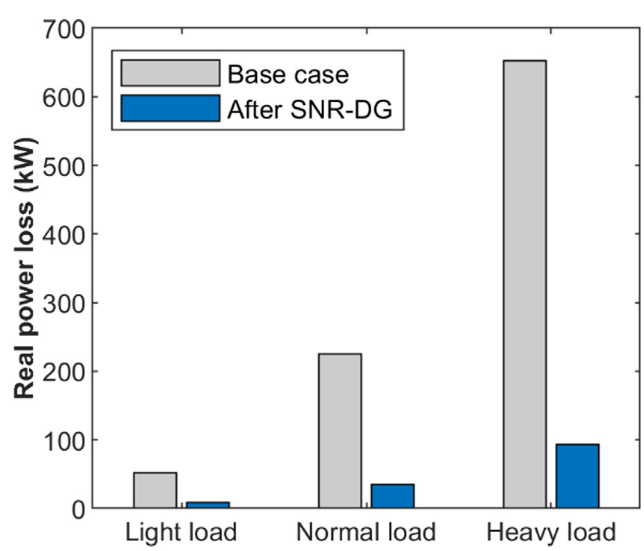


**Fig. 8** Real power loss of 69-bus RDN before and after SNR-DG at three load levels.

than those of SGA for all load levels. Hence, CSGA displayed better performance than the original SGA for solution quality.

Table 2 presents the comparison of outcomes obtained from the proposed CSGA with other methods at all load levels. At light load level, the CSGA recorded optimal opened switches (7-9-14-27-31), while the positions to install the DGs were at buses 12, 18, and 29 with sizes of 0.2384 MW, 0.3042 MW, and 0.5720 MW. CSGA offered minimum power

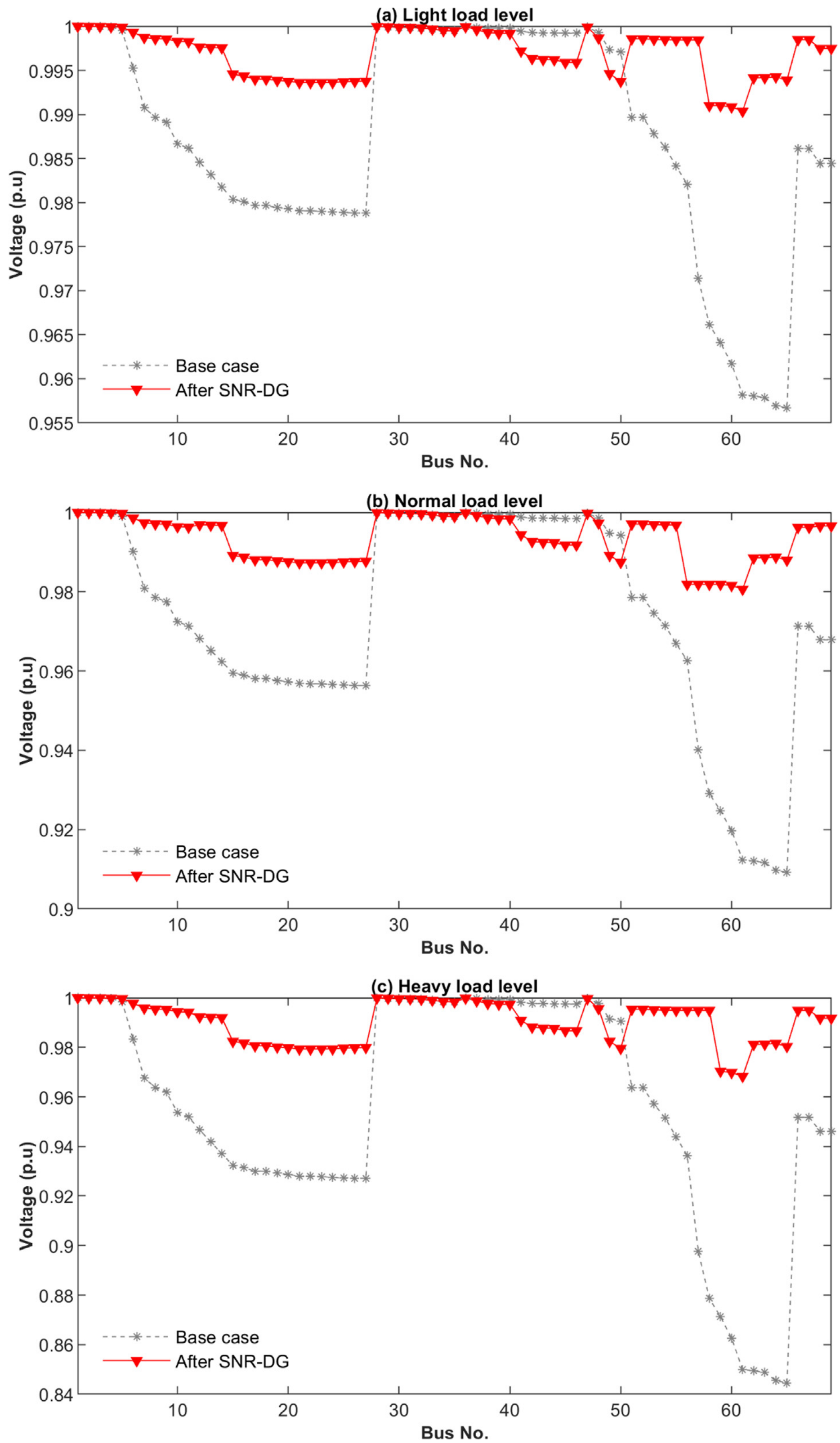


**Fig. 9** Voltage profiles of 69-bus RDN at three load levels.

loss (13.5232 kW) in comparison to other techniques. At normal load level, the CSGA optimized the system with opened switches (7-9-14-28-30), whereas the positions of DGs were at buses 12, 25, and 33 with sizes of 0.4697 MW, 1.0213 MW, and 0.7380 MW. The CSGA gave the best outcome with the lowest power loss (54.4788 kW), in comparison to SGA, MS, MBO, ACO, EOA [3], IEOA [3], HSA [17], GA [17], RGA [17], FWA [19], ISCA [27], and FF [28] at normal load level. At heavy load level, the CSGA offered NR with opened switches (7-9-14-27-31), wherein the DGs were connected to the positions at buses 12, 29, and 33 with sizes of 0.7722 MW, 1.8453 MW, and 0.9489 MW. The CSGA

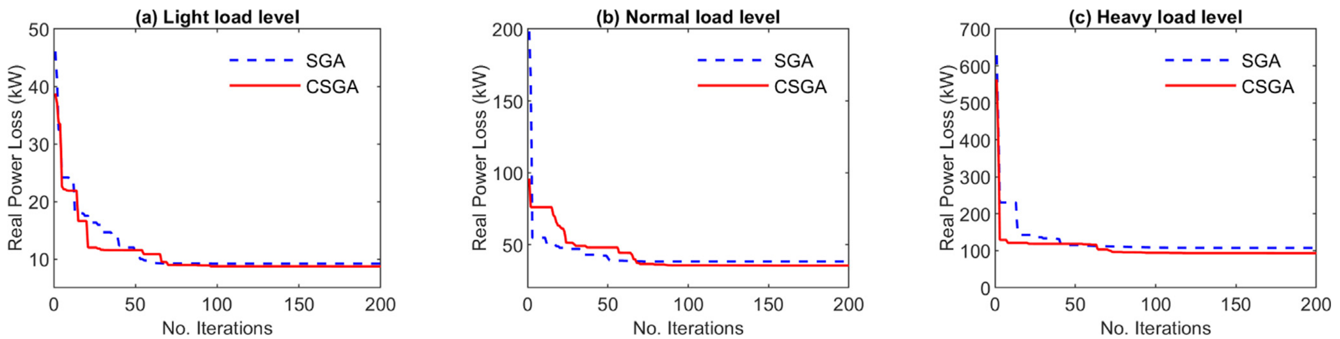


**Fig. 10** Convergence characteristics of CSGA and SGA for 69-bus RDN at three load levels.

**Table 4** Comparisons of CSGA and other methods for 69-bus RDN at three load levels.

| Loading level | Items | Opened switches | Sum $P_{DG}$ (kW) | $P_L$ (kW) | PLR (%) |
|---|---|---|---|---|---|
| Light loading level | Base case | 69-70-71-72-73 | - | 51.61 | - |
| | CSGA | 14-57-61-69-70 | 1.1406 | 8.7340 | 83.0757 |
| | SGA | 12-18-58-62-69 | 1.1406 | 9.1832 | 82.2053 |
| | MS | 10-12-56-64-70 | 1.1181 | 10.1225 | 80.3851 |
| | MBO | 13-25-56-69-70 | 1.0000 | 11.9662 | 76.8126 |
| | ACO | 10-13-55-61-71 | 1.0806 | 9.7316 | 81.1427 |
| | EOA [3] | 12-55-62-69-70 | 0.970 | 9.4497 | 81.76 |
| | IEOA [3] | 12-55-62-69-70 | 1.098 | 9.03737 | 81.83 |
| | HSA [17] | 10-14-16-56-62 | 1.0021 | 11.07 | 78.55 |
| | FWA [19] | 13-56-63-69-70 | 0.9399 | 9.58 | 81.43 |
| | ISCA [27] | 12-17-57-62-69 | 0.9721 | 10.02 | 80.58 |
| Normal loading level | Base case | 69-70-71-72-73 | – | 225 | – |
| | CSGA | 14-55-61-69-70 | 2.2813 | 35.3549 | 84.2867 |
| | SGA | 13-56-61-69-70 | 2.1001 | 38.2621 | 82.9946 |
| | MS | 9-13-18-57-61 | 2.2813 | 39.9384 | 82.2496 |
| | MBO | 13-57-62-69-70 | 2.0969 | 45.4028 | 79.8210 |
| | ACO | 14-54-63-69-70 | 2.2186 | 38.0079 | 83.1076 |
| | EOA [3] | 12-18-56-63-69 | 2.263 | 37.5495 | 83.31 |
| | IEOA [3] | 10-13-57-61-70 | 1.831 | 36.3986 | 83.82 |
| | HSA [17] | 13-17-58-61-69 | 1.8718 | 40.3 | 82.08 |
| | GA [17] | 10-15-45-55-62 | 2.0292 | 46.5 | 73.38 |
| | RGA [17] | 10-14-16-55-62 | 2.0654 | 44.23 | 80.32 |
| | FWA [19] | 13-55-63-69-70 | 1.8181 | 39.25 | 82.55 |
| | ISCA [27] | 12-19-57-63-69 | 1.8731 | 39.73 | 82.34 |
| | FF [28] | 12-19-57-61-69 | 1.9371 | 40.3 | 82.08 |
| Heavy loading level | Base case | 69-70-71-72-73 | – | 652.53 | – |
| | CSGA | 14-58-61-69-70 | 3.6500 | 93.1537 | 85.7241 |
| | SGA | 19-55-62-69-71 | 3.6500 | 107.7553 | 83.4864 |
| | MS | 12-14-56-63-69 | 3.3162 | 106.9845 | 83.6046 |
| | MBO | 14-55-69-70-73 | 3.0000 | 128.6349 | 80.2866 |
| | ACO | 16-57-63-69-71 | 3.6272 | 106.3824 | 83.6968 |
| | EOA [3] | 10-17-45-55-61 | 3.649 | 106.074 | 83.736 |
| | IEOA [3] | 10-12-13-57-62 | 3.649 | 100.4148 | 84.6 |
| | HSA [17] | 10-13-18-58-61 | 3.3828 | 104.67 | 83.96 |
| | FWA [19] | 13-57-63-69-70 | 2.9613 | 102.97 | 84.21 |
| | ISCA [27] | 14-55-62-69-70 | 2.7449 | 104.5 | 83.92 |

attained better outcomes than the rest of the techniques for the heavy load level. Hence, the proposed CSGA offered exceptional solution quality for 33-bus RDN.

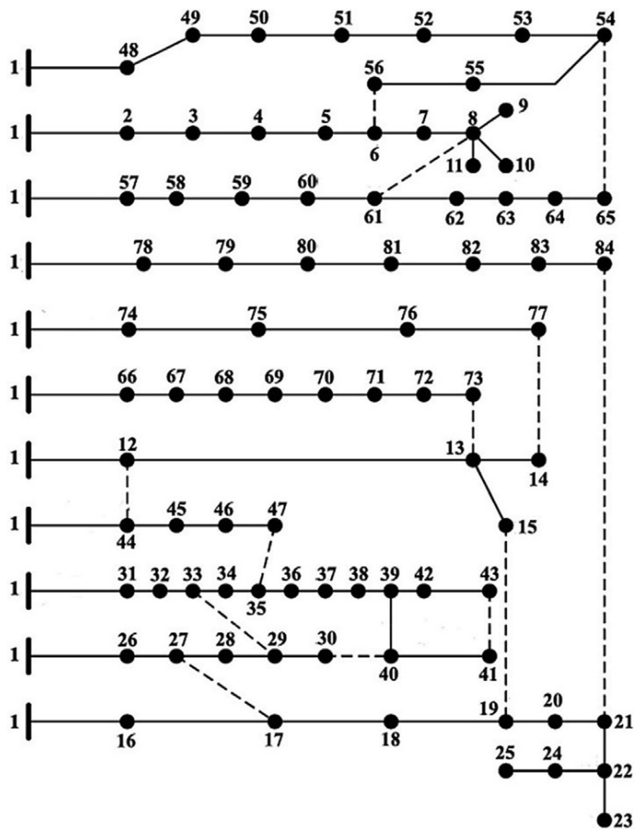

**Fig. 11** The IEEE 84-bus RDN.

### 5.2. 69-bus RDN

The IEEE 69-bus RDN denotes a medium-scale network with 73 branches, 5 opened switches, and 68 closed switches. The total load demand is 3.80 MW and 2.69 MVAr with a nominal voltage of 11.4 kV at normal load level. The branch and load data of this network are given in [43]. The initially opened switches were 69-70-71-72-73. Fig. 7 presents the diagram of the 69-bus RDN.

Table 3 tabulates the outcomes retrieved by CSGA and SGA for 69-bus RDN at three load levels. The base cases at light, normal, and heavy load levels had real power loss of

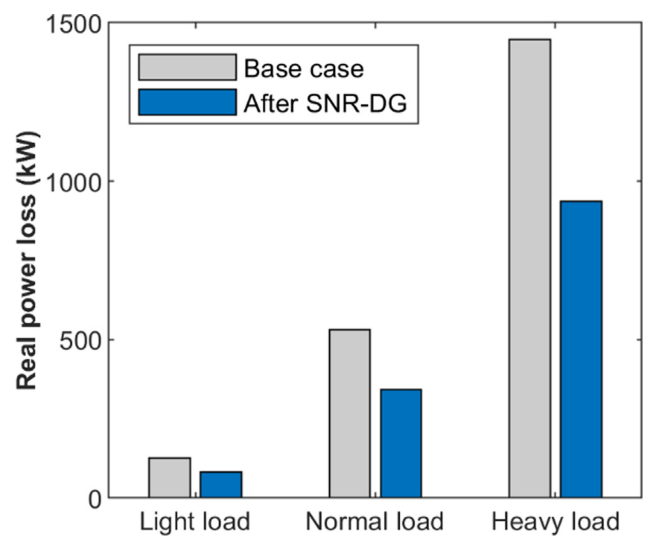


**Fig. 12** Real power loss of 84-bus RDN before and after SNR-DG at three load levels.

**Table 5** Optimal results of CSGA and SGA for 84-bus RDN at three load levels.

| Methods | Item | Load level | | |
|---|---|---|---|---|
| | | Light (0.5) | Normal (1) | Heavy (1.6) |
| Base case | Opened switches | 84-85-86-87-88-89-90-91-92-93-94-95-96 | 84-85-86-87-88-89-90-91-92-93-94-95-96 | 84-85-86-87-88-89-90-91-92-93-94-95-96 |
| | $P_L$ (kW) | 127.21 | 531.99 | 1446.50 |
| | $V_{min}$ (p.u) | 0.9657 | 0.9285 | 0.8787 |
| SGA | Opened switches | 6-32-39-41-54-64-72-81-86-88-89-90-94 | 7-14-32-34-37-42-55-63-72-83-86-88-90 | 7-32-34-38-41-62-72-82-84-86-88-89-90 |
| | $P_{DG}$ (MW)/ (Bus) | 1.6953/ (8)2.0434/ (20)1.9392/ (29) | 4.1368/ (20)2.6015/ (33)3.1325/ (80) | 4.9367/ (20)3.3531/ (29)4.0494/ (54) |
| | $P_L$ (kW) | 84.8942 | 365.0227 | 948.5959 |
| | PLR (%) | 33.2655 | 31.3860 | 34.4212 |
| | $V_{min}$ (p.u) | 0.9748 | 0.9517 | 0.9222 |
| CSGA | Opened switches | 34-39-62-72-81-84-85-86-88-89-90-92-95 | 7-33-39-42-61-70-84-86-88-89-90-91-92 | 39-41-55-81-85-86-87-88-89-90-92-94-96 |
| | $P_{DG}$ (MW)/ (Bus) | 1.5615/ (7)1.5374/ (65)1.5678/ (84) | 3.2512/ (54)3.6341/ (72)3.5853/ (80) | 5.0000/ (7)4.1286/ (72)4.6996/ (84) |
| | $P_L$ (kW) | 81.5048 | 342.2977 | 937.4880 |
| | PLR (%) | 35.9299 | 35.6577 | 35.1891 |
| | $V_{min}$ (p.u) | 0.9773 | 0.9561 | 0.9215 |

51.61 kW, 225 kW, and 652.53 kW, which decreased to 8.7340 kW, 35.3549 kW, and 93.1537 kW, respectively. The corresponding PLR values were 83.0757%, 84.2867%, and 85.7241% for light, normal, and heavy load levels. Fig. 8 portrays the real power loss of the 69-bus system before and after SNR-DG implementation using CSGA. Fig. 9 illustrates the

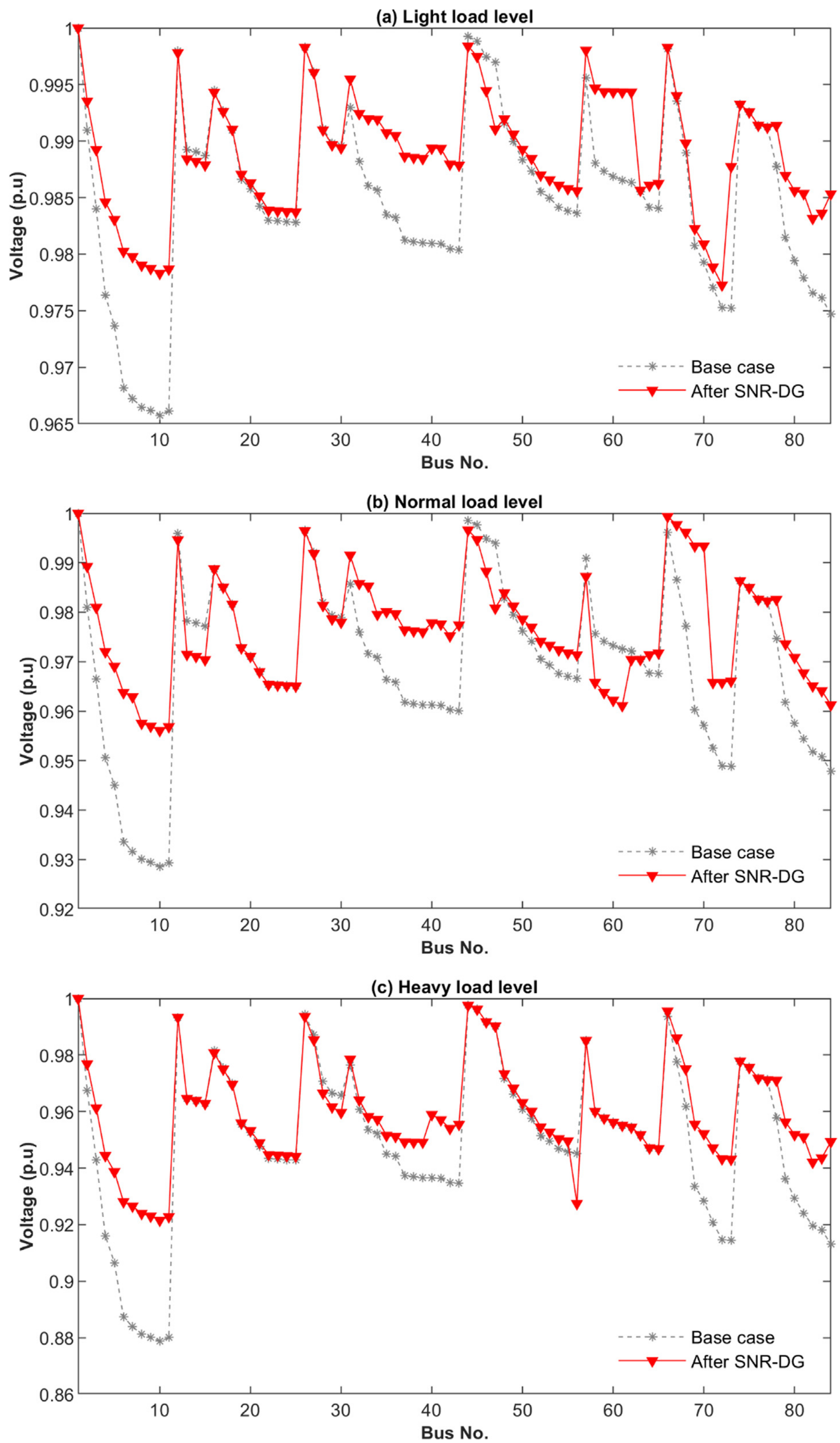


**Fig. 13** Voltage profiles of 84-bus RDN at three load levels.

voltage profile of 69-bus RDN at three load levels. Referring to Table 3 and Fig. 9, the minimum voltage magnitude enhanced from 0.9567p.u., 0.9092p.u., and 0.8445p.u. (base case) to 0.9904p.u., 0.9806p.u., and 0.9683p.u. at light, normal, and heavy load levels, respectively. Therefore, CSGA application for SNR-DG had successfully decreased real power loss and enhanced system voltage profile. Moreover, Fig. 10 displays that the CSGA achieved better convergence than SGA in all load levels.

Table 4 lists the comparative results between CSGA and the other methods for 69-bus RDN at three load levels. At light load level, CSGA optimized the NR with opened switches (14-57-61-69-70), while installation of DGs at buses 61, 64, and 66 with sizes of 0.6966 MW, 0.2338 MW, and 0.2102 MW, respectively. The real power loss achieved by CSGA was 8.7340 kW – the lowest when compared to all the other techniques (see Table 4). At normal load level, NR was defined with opened switches 14-55-61-69-70, while the DGs were connected to buses 12, 61, and 64 with sizes of 0.4062 MW, 1.4004 MW, and 0.4746 MW, respectively. The CSGA recorded lower power loss (35.3549 kW) when compared with SGA, MS, MBO, ACO, EOA [3], IEOA [3], HSA [17], GA [17], RGA [17], FWA [19], ISCA [27], and FF [28] for this load level. At heavy load level, CSGA displayed optimal NR with opened switches (14-58-61-69-70), whereas DGs placement at buses 61, 64, and 66 with sizes 2.2330 MW, 0.7557 MW, and 0.6613 MW, respectively. The real power loss recorded by CSGA was 93.1537 kW – the best yield among other methods for heavy load level. Thus, CSGA proved significantly superior performance to the other techinques for 69-bus RDN.

### 5.3. 84-bus RDN

The 84-bus RDN characterizes a practical distribution system of the Taiwan Power Company with 96 branches, 13 opened switches, and 83 closed switches [44]. At normal load level, the total load demand is 28.35 MW and 20.70 MVAr, and the nominal voltage of the system is 11.4 kV. The initially opened switches were 84-85-86-87-88-89-90-91-92-93-94-95-96. Fig. 11 shows the diagram of the 84-bus RDN.

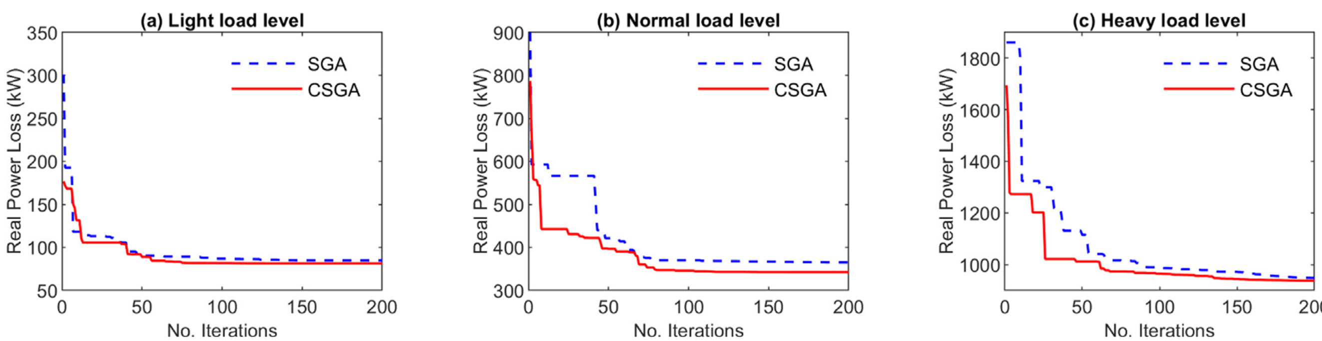


**Fig. 14** Convergence characteristics of CSGA and SGA for 84-bus RDN at three load levels.

**Table 6** Comparisons of CSGA and other methods for 84-bus RDN at three load levels.

| Loading level | Items | Opened switches | Sum $P_{DG}$ (MW) | $P_L$ (kW) | PLR (%) |
|---|---|---|---|---|---|
| Light loading level | Base case | 84-85-86-87-88-89-90-91-92-93-94-95-96 | - | 127.21 | - |
| | CSGA | 34-39-62-72-81-84-85-86-88-89-90-92-95 | 4.6668 | 81.5048 | 35.9299 |
| | SGA | 6-32-39-41-54-64-72-81-86-88-89-90-94 | 5.6779 | 84.8942 | 33.2655 |
| | MS | 33-53-72-82-84-85-86-88-89-90-92-93-95 | 5.1513 | 87.7448 | 31.0247 |
| | MBO | 33-39-63-83-84-85-86-87-88-89-90-92-95 | 3.7281 | 91.8226 | 27.8192 |
| | ACO | 36-42-54-64-80-85-86-87-88-89-90-92-94 | 4.7924 | 84.3741 | 33.6744 |
| Normal loading level | Base case | 84-85-86-87-88-89-90-91-92-93-94-95-96 | - | 531.99 | - |
| | CSGA | 7-33-39-42-61-70-84-86-88-89-90-91-92 | 10.4706 | 342.2977 | 35.6577 |
| | SGA | 7-14-32-34-37-42-55-63-72-83-86-88-90 | 9.8708 | 365.0227 | 31.3860 |
| | MS | 7-34-38-40-54-61-72-76-83-86-89-90-92 | 10.1316 | 372.7662 | 29.9304 |
| | MBO | 36-54-70-81-85-86-88-89-90-92-94-95-96 | 15.0000 | 371.0536 | 30.2524 |
| | ACO | 34-38-41-72-76-84-85-86-89-90-91-92-96 | 9.5284 | 360.1071 | 32.3100 |
| Heavy loading level | Base case | 84-85-86-87-88-89-90-91-92-93-94-95-96 | - | 1446.50 | - |
| | CSGA | 39-41-55-81-85-86-87-88-89-90-92-94-96 | 13.8282 | 937.4880 | 35.1891 |
| | SGA | 7-32-34-38-41-62-72-82-84-86-88-89-90 | 12.3391 | 948.5959 | 34.4212 |
| | MS | 13-33-36-64-72-82-84-85-86-89-90-92-95 | 13.3035 | 963.2455 | 33.4084 |
| | MBO | 33-39-55-76-81-85-86-87-89-90-92-95-96 | 15.0000 | 944.5001 | 34.7043 |
| | ACO | 33-37-55-64-83-85-86-87-88-89-90-92-95 | 15 | 940.0672 | 35.0108 |

Table 5 gives the results yielded by CSGA and SGA for different load levels. As for the base case at light, nominal, and heavy load levels, the system had real power losses of 127.21 kW, 531.99 kW, and 1446.50 kW with minimum voltages of 0.9657p.u., 0.9285p.u., and 0.8787p.u., respectively. After optimization, the real power losses were reduced to 81.5048 kW (35.9299% PLR), 342.2977 kW (35.6577% PLR), and 937.4880 kW (35.1891% PLR), respectively. Furthermore, the minimum voltage magnitude had enhanced to 0.9773p.u., 0.9561p.u., and 0.9215p.u. at light, normal, and heavy load levels, respectively. Fig. 12 depicts the real power loss of 84-bus RDN before and after SNR-DG implementation using CSGA. The voltage profiles of all load levels are also portrayed in Fig. 13. It can be concluded that real power loss and system voltage profile were improved after SNR-DG using CSGA. Furthermore, convergence characteristics of CSGA were also better than SGA in all load levels, as shown in Fig. 14.

As can be seen in Table 6, the proposed CSGA was compared with SGA, MS, MBO, ACO methods for this system. From Table 6, CSGA yielded a better result (81.5048 kW) than other techniques for the light load level. At normal load level, CSGA found minimum power loss (342.2977 kW) when compared to SGA, MS, MBO, and ACO. At heavy load level, CSGA found the best outcome with the lowest power loss (937.4880 kW), in comparison to the rest of the techniques. Therefore, the proposed CSGA proved its efficiencies in finding exceptional solution quality for 84-bus RDN.

### *5.4. 118-bus RDN*

The IEEE 118-bus RDN represents a large-scale network with 132 branches, 15 opened switches, and 117 closed switches [45]. At normal load level, the total load demand is 22.71 MW and 17.04 MVAr, and the nominal voltage of the system is 11 kV. The initially opened switches were 118-119-120-121-122-123-124-125-126-127-128-129-130-131-132. Fig. 15 shows the diagram of the 118-bus RDN.

The results found by CSGA and SGA for different load levels are reported in Table 7. As for the base case, the real power loss of the system at light, normal, and heavy load levels were 297.15 kW, 1298.09 kW, and 3799.70 kW, respectively, which reduced to 134.9253 kW (54.5933% PLR), 467.0906 kW (64.0171% PLR), and 1299.6690 kW (65.7955% PLR), respectively, after CSGA implementation for SNR-DG. Fig. 16 depicts the real power loss of the 118-

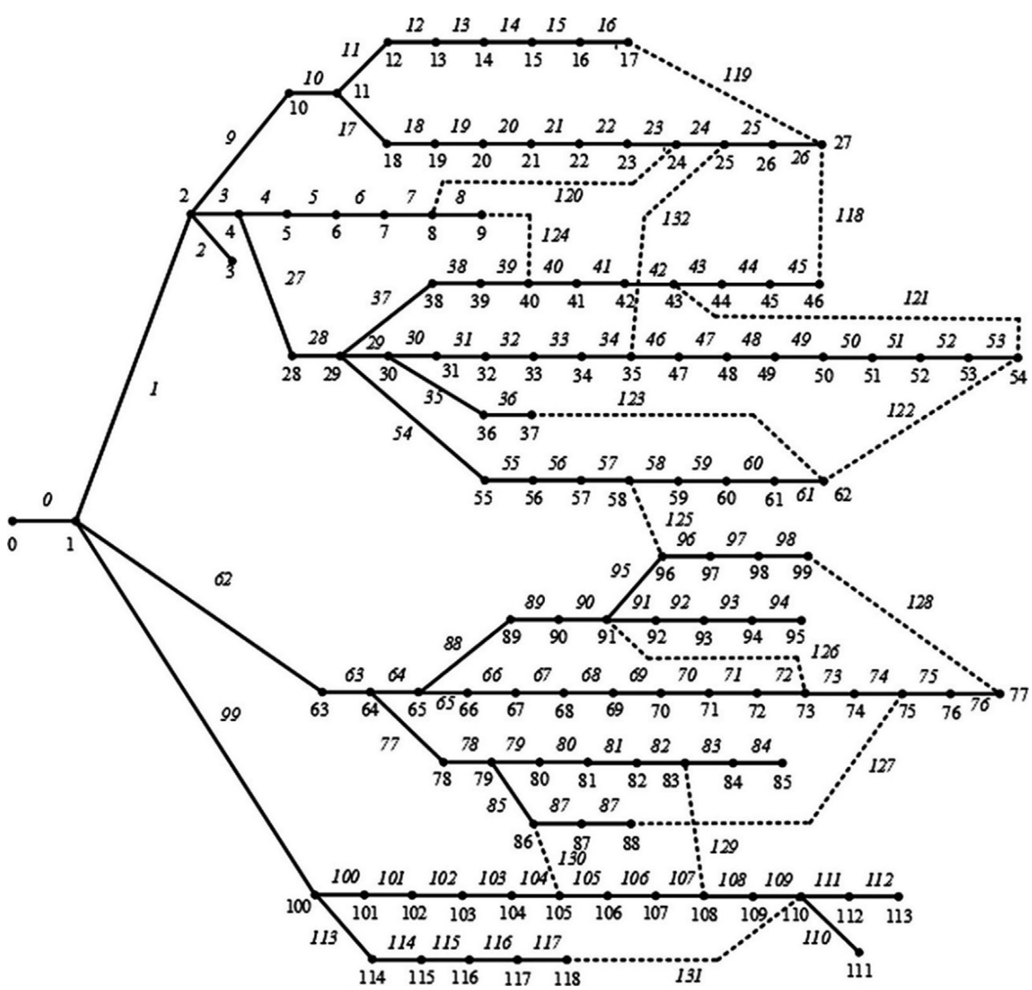

**Fig. 15** The IEEE 118-bus RDN.

**Table 7** Optimal results of CSGA and SGA for 118-bus RDN at three load levels.

| Methods | Item | Load level | | |
|---|---|---|---|---|
| | | Light (0.5) | Normal (1) | Heavy (1.6) |
| Base case | Opened switches | 118-119-120-121-122-123-124-125-126-127-128-129-130-131-132 | 118-119-120-121-122-123-124-125-126-127-128-129-130-131-132 | 118-119-120-121-122-123-124-125-126-127-128-129-130-131-132 |
| | $P_L$ (kW) | 297.15 | 1298.09 | 3799.70 |
| | $V_{min}$ (p.u) | 0.9385 | 0.8688 | 0.7673 |
| SGA | Opened switches | 15-23-34-39-40-52-59-71-86-89-104-107-109-121-128 | 6-21-24-26-44-51-66-82-90-95-108-121-123-128-130 | 11-22-34-39-51-54-72-81-118-122-125-126-128-130-131 |
| | $P_{DG}$ (MW)/ (Bus) | 2.6756/ (4)<br>0.8973/ (8)<br>0.9418/ (27)<br>0.6813/ (70)<br>0.7954/ (74)<br>0.1135/ (92)<br>0.7080/ (96) | 1.5431/ (4)<br>1.4231/ (25)<br>0.8279/ (34)<br>1.2396/ (42)<br>2.6673/ (58)<br>1.4166/ (64)<br>3.4797/ (73) | 2.5410/ (9)<br>1.5572/ (25)<br>2.2676/ (43)<br>1.6052/ (58)<br>1.4562/ (88)<br>3.9502/ (96)<br>4.4897/ (110) |
| | $P_L$ (kW) | 178.2864 | 742.9589 | 1663.3932 |
| | PLR (%) | 40.0009 | 42.7653 | 56.2231 |
| | $V_{min}$ (p.u) | 0.9667 | 0.9121 | 0.9066 |
| CSGA | Opened switches | 15-22-34-39-42-45-48-58-70-82-86-95-104-109-128 | 21-25-34-39-42-53-61-72-85-95-98-107-109-123-127 | 22-26-33-39-45-53-61-72-81-87-109-123-125-128-130 |
| | $P_{DG}$ (MW)/ (Bus) | 0.9027/ (31)<br>0.4957/ (42)<br>1.0649/ (51)<br>1.1621/(74)<br>1.3602/ (79)<br>0.5993/ (83)<br>0.8315/ (96) | 2.1969/ (50)<br>1.6267/ (70)<br>2.8873/ (81)<br>1.4496/ (97)<br>1.0702/ (99)<br>1.8278/ (105)<br>1.4913/ (111) | 3.1402/ (42)<br>3.4853/ (50)<br>1.6731/ (71)<br>0.9286/ (76)<br>2.3376/ (83)<br>4.1690/ (96)<br>4.2231/ (118) |
| | $P_L$ (kW) | 134.9253 | 467.0906 | 1299.6690 |
| | $PLR$ (%) | 54.5933 | 64.0171 | 65.7955 |
| | $V_{min}$ (p.u) | 0.9678 | 0.9570 | 0.9503 |

bus system before and after SNR-DG implementation using CSGA. The voltage profile improvements of all load levels are shown in Fig. 17. Accordingly, the minimum voltage magnitude had enhanced from 0.9385p.u., 0.8688p.u., and 0.7673p.u. (base case) to 0.9678p.u., 0.9570p.u., and 0.9503p.u. at light, normal, and heavy load levels, respectively. This indicated that the CSGA application for SNR-DG had successfully improved the system performance in terms of reduced real power loss and enhanced system voltage profile. As for the convergence curves in Fig. 18, CSGA obtained better optimal solutions at faster convergence than SGA at all load levels.

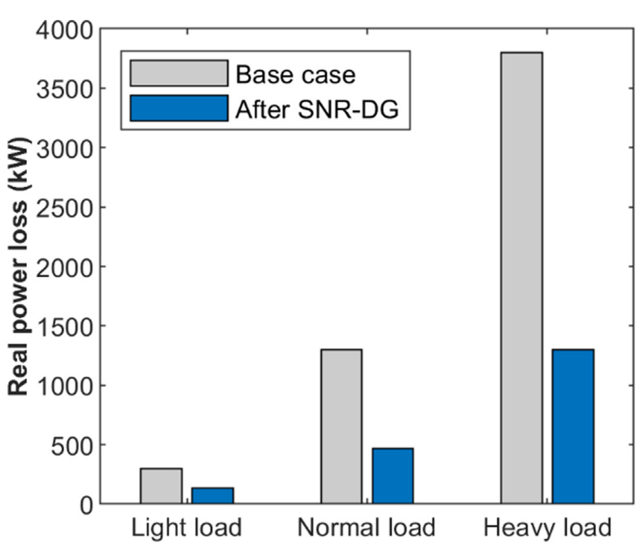


**Fig. 16** Real power loss of 118-bus RDN before and after SNR-DG at three load levels.

Table 8 presents the comparisons of CSGA and the other methods for 118-bus RDN at three load levels. At light load level, the real power loss recorded by CSGA was 134.9253 kW – the best yield among other methods. At normal load level, the CSGA recorded lower power loss (467.0906 kW) when compared with SGA (742.9589 kW), MS (644.3031 kW), MBO (853.5588 kW), and ACO (854.8006 kW). Moreover, the real power loss achieved by CSGA was 1299.6690 kW – the lowest when compared to all the other techniques.

CSGA shows high exploration and exploitation. The superior exploration of CSGA is due to the updating solutions around a set of best solutions obtained so far (i.e., search group members). CSGA can explore the search space more extensively and find more promising regions. The high exploration of CSGA also benefits from the mutation process, which helps to drive the algorithm to discover newer regions of the search domain and avoid the local optimum in each iteration. Another advantage is the high exploitation of CSGA, which is because of both perturbation coefficient in family

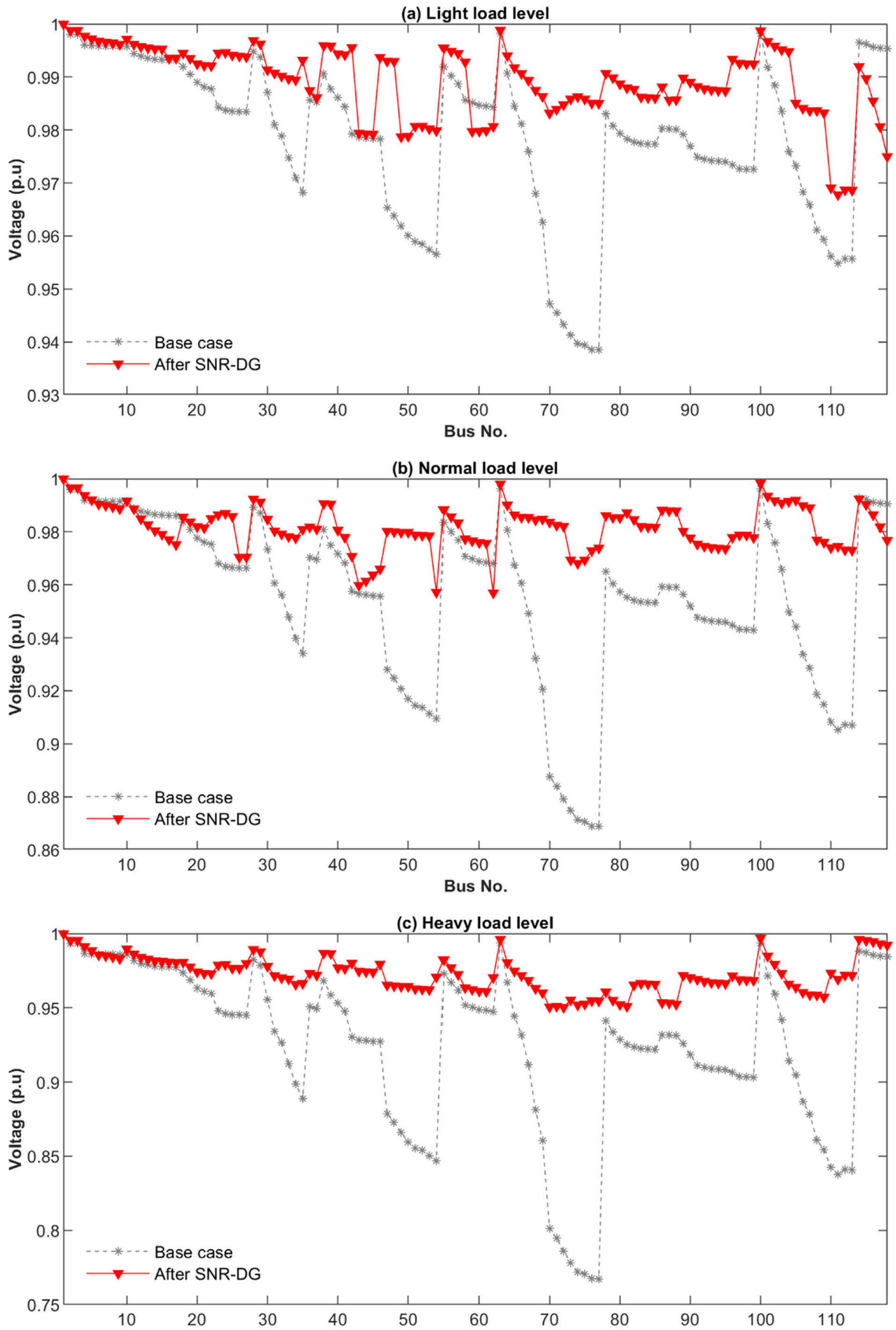


**Fig. 17** Voltage profiles of 118-bus RDN at three load levels.

generation and the new search group selection mechanism. CSGA uses the perturbation coefficient ($\alpha$) for a smooth transition from exploration to exploitation in the optimization process. When the perturbation coefficient has a high value in the first iterations, CSGA generates individuals spreading throughout the design space. When the perturbation coefficient is adaptively reduced over iterations, individuals created by CSGA tend to locate in their neighborhood. Furthermore, new search group selection is done by two different mechanisms in global and local phases for generating a good balance between exploitation and exploration capabilities of CSGA. Thanks to the integration of the CLS strategy, CSGA has the advantage of improving the search performance and avoiding being stuck in the local optimum. Accordingly, the

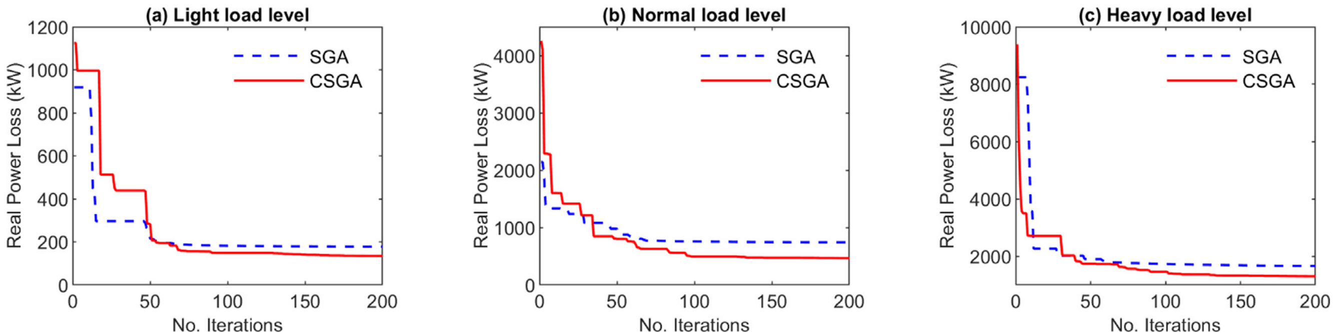


**Fig. 18** Convergence characteristics of CSGA and SGA for 118-bus RDN at three load levels.

**Table 8** Comparisons of CSGA and other methods for 118-bus RDN at three load levels.

| Loading level | Items | Opened switches | Sum $P_{DG}$ (MW) | $P_L$ (kW) | PLR (%) |
|---|---|---|---|---|---|
| Light loading level | Base case | 118-119-120-121-122-123-124-125-126-127-128-129-130-131-132 | - | 297.15 | - |
| | CSGA | 15-22-34-39-42-45-48-58-70-82-86-95-104-109-128 | 6.4163 | 134.9253 | 54.5933 |
| | SGA | 15-23-34-39-40-52-59-71-86-89-104-107-109-121-128 | 6.8129 | 178.2864 | 40.0009 |
| | MS | 5-21-25-44-58-66-75-80-86-108-121-122-124-125-130 | 6.1226 | 167.6298 | 33.8970 |
| | MBO | 41-53-109-119-120-122-123-124-125-126-127-128-129-130-132 | 5.9555 | 207.3185 | 30.2307 |
| | ACO | 7-15-60-72-97-116-118-120-121-123-125-127-129-130-132 | 2.7223 | 209.2329 | 29.5864 |
| Normal loading level | Base case | 118-119-120-121-122-123-124-125-126-127-128-129-130-131-132 | – | 1298.09 | – |
| | CSGA | 21-25-34-39-42-53-61-72-85-95-98-107-109-123-127 | 12.5497 | 467.0906 | 64.0171 |
| | SGA | 6-21-24-26-44-51-66-82-90-95-108-121-123-128-130 | 12.5973 | 742.9589 | 42.7653 |
| | MS | 8-24-26-60-66-74-82-95-109-119-120-121-122-127-130 | 13.4289 | 644.3031 | 50.3654 |
| | MBO | 42-53-119-120-122-123-124-125-126-127-128-129-130-131-132 | 11.9001 | 853.5588 | 34.2451 |
| | ACO | 15-21-39-42-53-59-88-97-122-126-127-129-130-131-132 | 12.5862 | 854.8006 | 34.1494 |
| Heavy loading level | Base case | 118-119-120-121-122-123-124-125-126-127-128-129-130-131-132 | – | 3799.70 | – |
| | CSGA | 22-26-33-39-45-53-61-72-81-87-109-123-125-128-130 | 19.9569 | 1299.6690 | 65.7955 |
| | SGA | 11-22-34-39-51-54-72-81-118-122-125-126-128-130-131 | 17.8671 | 1663.3932 | 56.2231 |
| | MS | 11-20-33-41-53-58-72-81-98-108-118-124-125-127-130 | 20.2432 | 1560.7025 | 58.9257 |
| | MBO | 45-107-119-120-121-122-123-124-125-126-127-128-129-130-132 | 21.0000 | 1827.8675 | 51.8945 |
| | ACO | 17-33-39-42-52-59-72-89-98-109-119-122-126-129-130 | 15.0215 | 1918.2644 | 49.5154 |

exploitation ability of CSGA is significantly improved. Hence, CSGA obtained very competitive results and tended to outperform other compared methods for the SNR-DG problem.

## 6. Conclusion

The proposed CSGA approach had been successfully deployed in this study to address the SNR-DG problem in RDNs. The CSGA incorporated a chaotic local search into the original SGA to enhance its search performance. The CSGA is, indeed, a powerful search metaheuristic approach that deals with optimization problems with exceptional solution quality and high convergence speed. In this study, the CSGA was applied to 33-, 69-, 84-, and 118-bus RDNs to attain PLR maximization for three load levels (light load: 0.5, normal load: 1.0, and heavy load: 1.6) for the SNR-DG problem. The outcomes revealed the capability exerted by CSGA in handling complex and large-scale RDNs. For all load levels, CSGA recorded the best solution quality when compared to other existing approaches for PLR. Therefore, the CSGA proposed in this study stands as an effective technique to address the SNR-DG problem. For future works, the SNR-DG problem may be formulated as a multi-objective problem considering technical and economic aspects. Moreover, it is encouraging to develop a multi-objective version of CSGA to solve the multi-objective problems in power systems.

## Declaration of Competing Interest

The authors declare that they have no known competing financial interests or personal relationships that could have appeared to influence the work reported in this paper.


## Acknowledgments

We acknowledge the support of time and facilities from Ho Chi Minh City University of Technology (HCMUT), VNU-HCM for this study.

## References


[1] S. Gopiya Naik, D.K. Khatod, M.P. Sharma, Optimal allocation of combined DG and capacitor for real power loss minimization in distribution networks, Int. J. Electr. Power Energy Syst. 53 (2013) 967–973, https://doi.org/10.1016/j.ijepes.2013.06.008.

[2] T. Tran The, B.-H. Truong, K. Dang Tuan, D. Vo Ngoc, C.M. Chen, Vo Ngoc, A Nondominated Sorting Stochastic Fractal Search Algorithm for Multiobjective Distribution Network Reconfiguration with Distributed Generations, Math. Problems Eng. 2021 (2021) 1–20, https://doi.org/10.1155/2021/6638559.

[3] A.M. Shaheen, A.M. Elsayed, R.A. El-Sehiemy, A.Y. Abdelaziz, Equilibrium optimization algorithm for network reconfiguration and distributed generation allocation in power systems, Appl. Soft Comput. 98 (2021) 106867, https://doi.org/10.1016/j.asoc.2020.106867.

[4] S. Mishra, D. Das, S. Paul, A comprehensive review on power distribution network reconfiguration, Energy Syst. 8 (2) (2017) 227–284, https://doi.org/10.1007/s12667-016-0195-7.

[5] M.A. Kashem, G.B. Jasmon, V. Ganapathy, A new approach of distribution system reconfiguration for loss minimization, Int. J. Electr. Power Energy Syst. 22 (4) (2000) 269–276, https://doi.org/10.1016/S0142-0615(99)00057-5.

[6] T.E. McDermott, I. Drezga, R.P. Broadwater, A heuristic nonlinear constructive method for distribution system reconfiguration, IEEE Trans. Power Syst. 14 (2) (1999) 478–483, https://doi.org/10.1109/59.761869.

[7] F.V. Gomes, S. Carneiro, J.L.R. Pereira, M.P. Vinagre, P.A.N. Garcia, L.R. Araujo, A new heuristic reconfiguration algorithm for large distribution systems, IEEE Trans. Power Syst. 20 (3) (2005) 1373–1378, https://doi.org/10.1109/TPWRS.2005.851937.

[8] A.M. Othman, A.A. El-Fergany, A.Y. Abdelaziz, Optimal Reconfiguration Comprising Voltage Stability Aspect Using Enhanced Binary Particle Swarm Optimization Algorithm, Electr. Power Compon. Syst. 43 (14) (2015) 1656–1666, https://doi.org/10.1080/15325008.2015.1041623.

[9] J.Z. Zhu, Optimal reconfiguration of electrical distribution network using the refined genetic algorithm, Electr. Power Syst. Res. 62 (1) (2002) 37–42, https://doi.org/10.1016/S0378-7796(02)00041-X.

[10] R. Srinivasa Rao, S.V.L. Narasimham, M. Ramalinga Raju, A. Srinivasa Rao, Optimal Network Reconfiguration of Large-Scale Distribution System Using Harmony Search Algorithm, IEEE Trans. Power Syst. 26 (3) (2011) 1080–1088, https://doi.org/10.1109/TPWRS.2010.2076839.

[11] A. Mohamed Imran, M. Kowsalya, A new power system reconfiguration scheme for power loss minimization and voltage profile enhancement using Fireworks Algorithm, Int. J. Electr. Power Energy Syst. 62 (2014) 312–322, https://doi.org/10.1016/j.ijepes.2014.04.034.

[12] T.T. Nguyen, A.V. Truong, Distribution network reconfiguration for power loss minimization and voltage profile improvement using cuckoo search algorithm, Int. J. Electr. Power Energy Syst. 68 (2015) 233–242, https://doi.org/10.1016/j.ijepes.2014.12.075.

[13] C.-H. Chen, C.-Y. Lu, T.-P. Hong, J.-W. Lin, M. Gaeta, An Effective Approach for the Diverse Group Stock Portfolio Optimization Using Grouping Genetic Algorithm, IEEE Access 7 (2019) 155871–155884, https://doi.org/10.1109/ACCESS.2019.2949055.

[14] Y. Shao, J.-C.-W. Lin, G. Srivastava, D. Guo, H. Zhang, H. Yi, A. Jolfaei, Multi-Objective Neural Evolutionary Algorithm for Combinatorial Optimization Problems, IEEE Trans. Neural Networks Learn. Syst. (2021) 1–11, https://doi.org/10.1109/TNNLS.2021.3105937.

[15] T.D. Pham, T.T. Nguyen, B.H. Dinh, Find optimal capacity and location of distributed generation units in radial distribution networks by using enhanced coyote optimization algorithm, Neural Comput. Appl. 33 (9) (2021) 4343–4371, https://doi.org/10.1007/s00521-020-05239-1.

[16] M. Esmaeili, M. Sedighizadeh, M. Esmaili, Multi-objective optimal reconfiguration and DG (Distributed Generation) power allocation in distribution networks using Big Bang-Big Crunch algorithm considering load uncertainty, Energy 103 (2016) 86–99, https://doi.org/10.1016/j.energy.2016.02.152.

[17] R.S. Rao, K. Ravindra, K. Satish, S.V.L. Narasimham, Power Loss Minimization in Distribution System Using Network Reconfiguration in the Presence of Distributed Generation, IEEE Trans. Power Syst. 28 (2013) 317–325, https://doi.org/10.1109/TPWRS.2012.2197227.

[18] M.F. Abd El-salam, E. Beshr, M.B. Eteiba, A New Hybrid Technique for Minimizing Power Losses in a Distribution System by Optimal Sizing and Siting of Distributed Generators with Network Reconfiguration, Energies 11 (2018) 3351, https://doi.org/10.3390/en11123351.

[19] A. Mohamed Imran, M. Kowsalya, D.P. Kothari, A novel integration technique for optimal network reconfiguration and distributed generation placement in power distribution networks, Int. J. Electr. Power Energy Syst. 63 (2014) 461–472, https://doi.org/10.1016/j.ijepes.2014.06.011.

[20] T.T. Nguyen, A.V. Truong, T.A. Phung, A novel method based on adaptive cuckoo search for optimal network reconfiguration and distributed generation allocation in distribution network, Int. J. Electr. Power Energy Syst. 78 (2016) 801–815, https://doi.org/10.1016/j.ijepes.2015.12.030.

[21] A. Onlam, D. Yodphet, R. Chatthaworn, C. Surawanitkun, A. Siritaratiwat, P. Khunkitti, Power Loss Minimization and Voltage Stability Improvement in Electrical Distribution System via Network Reconfiguration and Distributed Generation Placement Using Novel Adaptive Shuffled Frogs Leaping Algorithm, Energies 12 (2019) 553, https://doi.org/10.3390/en12030553.

[22] Z. Gong, Q. Chen, K. Sun, Novel methodology solving distribution network reconfiguration with DG placement, J. Eng. 2019 (16) (2019) 1668–1674, https://doi.org/10.1049/joe.2018.8521.

[23] H.B. Tolabi, M.H. Ali, Shahrin Bin Md Ayob, M. Rizwan, Novel hybrid fuzzy-Bees algorithm for optimal feeder multi-objective reconfiguration by considering multiple-distributed generation, Energy 71 (2014) 507–515, https://doi.org/10.1016/j.energy.2014.04.099.

[24] M. K., J. S., Integrated approach of network reconfiguration with distributed generation and shunt capacitors placement for power loss minimization in radial distribution networks, Appl. Soft Comput. 52 (2017) 1262–1284, https://doi.org/10.1016/j.asoc.2016.07.031.

[25] R. Rajaram, K. Sathish Kumar, N. Rajasekar, Power system reconfiguration in a radial distribution network for reducing losses and to improve voltage profile using modified plant growth simulation algorithm with Distributed Generation (DG), Energy Rep. 1 (2015) 116–122, https://doi.org/10.1016/j.egyr.2015.03.002.

[26] A. Bayat, A. Bagheri, R. Noroozian, Optimal siting and sizing of distributed generation accompanied by reconfiguration of distribution networks for maximum loss reduction by using a new UVDA-based heuristic method, Int. J. Electr. Power Energy Syst. 77 (2016) 360–371, https://doi.org/10.1016/j.ijepes.2015.11.039.

[27] U. Raut, S. Mishra, An improved sine–cosine algorithm for simultaneous network reconfiguration and DG allocation in power distribution systems, Appl. Soft Comput. 92 (2020) 106293, https://doi.org/10.1016/j.asoc.2020.106293.

[28] O. Badran, H. Mokhlis, S. Mekhilef, W. Dahalan, J. Jallad, Minimum switching losses for solving distribution NR problem with distributed generation, IET Gener. Transm. Distrib. 12 (8) (2018) 1790–1801, https://doi.org/10.1049/iet-gtd.2017.0595.

[29] M.S. Gonçalves, R.H. Lopez, L.F.F. Miguel, Search group algorithm: A new metaheuristic method for the optimization of truss structures, Comput. Struct. 153 (2015) 165–184, https://doi.org/10.1016/j.compstruc.2015.03.003.

[30] G.-G. Wang, S. Deb, A.H. Gandomi, Z. Zhang, A.H. Alavi, Chaotic cuckoo search, Soft Comput. 20 (9) (2016) 3349–3362, https://doi.org/10.1007/s00500-015-1726-1.

[31] G.G. Wang, S. Deb, A.H. Gandomi, Z. Zhang, A.H. Alavi, A Novel Cuckoo Search with Chaos Theory and Elitism Scheme, Int. Conf. Soft Comput. Mach. Intell. 2014 (2014) 64–69, https://doi.org/10.1109/ISCMI.2014.8.

[32] G.-G. Wang, L. Guo, A.H. Gandomi, G.-S. Hao, H. Wang, Chaotic Krill Herd algorithm, Inf. Sci. 274 (2014) 17–34, https://doi.org/10.1016/j.ins.2014.02.123.

[33] G.-G. Wang, A. Hossein Gandomi, A. Hossein Alavi, A chaotic particle-swarm krill herd algorithm for global numerical optimization, Kybernetes 42 (6) (2013) 962–978, https://doi.org/10.1108/K-11-2012-0108.

[34] S. Saha, V. Mukherjee, Optimal placement and sizing of DGs in RDS using chaos embedded SOS algorithm, IET Gener. Transm. Distrib. 10 (14) (2016) 3671–3680, https://doi.org/10.1049/iet-gtd.2016.0151.

[35] S. Saha, V. Mukherjee, A novel chaos-integrated symbiotic organisms search algorithm for global optimization, Soft Comput. 22 (11) (2018) 3797–3816, https://doi.org/10.1007/s00500-017-2597-4.

[36] S. Saha, V. Mukherjee, A novel quasi-oppositional chaotic antlion optimizer for global optimization, Appl. Intell. 48 (9) (2018) 2628–2660, https://doi.org/10.1007/s10489-017-1097-7.

[37] A.Y. Abdelaziz, F.M. Mohamed, S.F. Mekhamer, M.A.L. Badr, Distribution system reconfiguration using a modified Tabu Search algorithm, Electr. Power Syst. Res. 80 (8) (2010) 943–953, https://doi.org/10.1016/j.epsr.2010.01.001.

[38] M. Heidarifar, P. Andrianesis, M. Caramanis, A Riemannian optimization approach to the radial distribution network load flow problem, Automatica 129 (2021) 109620, https://doi.org/10.1016/j.automatica.2021.109620.

[39] T. Xiang, X. Liao, K.-w. Wong, An improved particle swarm optimization algorithm combined with piecewise linear chaotic map, Appl. Math. Comput. 190 (2) (2007) 1637–1645, https://doi.org/10.1016/j.amc.2007.02.103.

[40] G.-G. Wang, Moth search algorithm: a bio-inspired metaheuristic algorithm for global optimization problems, Memetic Comp. 10 (2) (2018) 151–164, https://doi.org/10.1007/s12293-016-0212-3.

[41] Y. Feng, S. Deb, G.-G. Wang, A.H. Alavi, Monarch butterfly optimization: A comprehensive review, Expert Syst. Appl. 168 (2021) 114418, https://doi.org/10.1016/j.eswa.2020.114418.

[42] M. Dorigo, M. Birattari, T. Stutzle, Ant colony optimization artificial ants as a computational intelligence technique, IEEE Comput. Intell. Mag. 1 (4) (2006) 28–39, https://doi.org/10.1109/CI-M.2006.248054.

[43] M.E. Baran, F.F. Wu, Network reconfiguration in distribution systems for loss reduction and load balancing, IEEE Trans. Power Delivery 4 (1989) 1401–1407, https://doi.org/10.1109/61.25627.

[44] S.u. Ching-Tzong, C.-S. Lee, Network reconfiguration of distribution systems using improved mixed-integer hybrid differential evolution, IEEE Trans. Power Delivery 18 (2003) 1022–1027, https://doi.org/10.1109/TPWRD.2003.813641.

[45] D. Zhang, Z. Fu, L. Zhang, An improved TS algorithm for loss-minimum reconfiguration in large-scale distribution systems, Electr. Power Syst. Res. 77 (5-6) (2007) 685–694, https://doi.org/10.1016/j.epsr.2006.06.005.